Title
MASS TRANSFER LIMITING CURRENTS OF ZINC DEPOSITION IN ACIDIC ZnCl2 AND ZnSO4 SOLUTIONS

Authors
Rajhenbah, D.
Faltemier, J.
Tobias, C.W.

Publication Date
1983-10-01

Lawrence Berkeley Laboratory
UNIVERSITY OF CALIFORNIA

Materials & Molecular Research Division

To be submitted for publication

MASS TRANSFER LIMITING CURRENTS OF ZINC DEPOSITION IN ACIDIC $ZnCl_2$ AND $ZnSO_4$ SOLUTIONS

D. Rajhenbah, J. Faltemier, and C.W. Tobias

October 1983

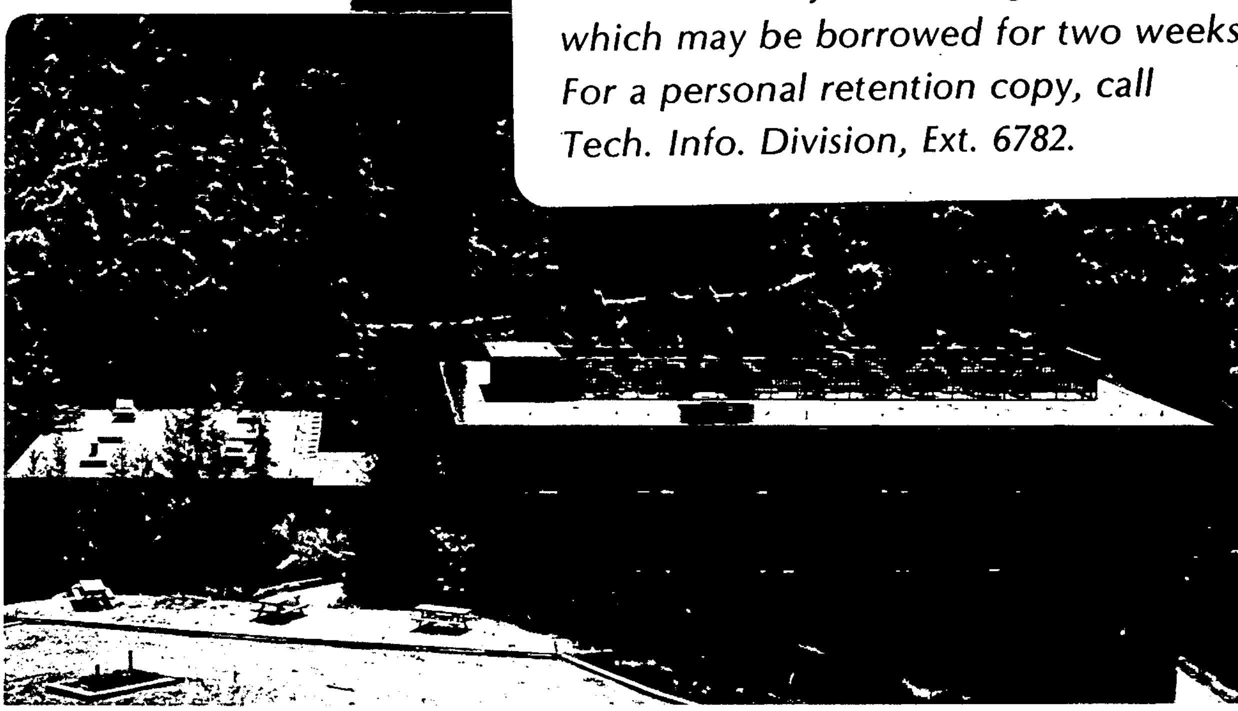

Prepared for the U.S. Department of Energy under Contract DE-AC03-76SF00098

DISCLAIMER

LBL-15338

MASS TRANSFER LIMITING CURRENTS OF ZINC DEPOSITION IN ACIDIC $ZnCl_2$ and $ZnSO_4$ SOLUTIONS

D. Rajhenbah*, J. Faltemier and C. W. Tobias

Materials and Molecular Research Division,
Lawrence Berkeley Laboratory
and Department of Chemical Engineering
University of California, Berkeley, CA 94720 USA

This work was supported by the Assistant Secretary for Conservation and Renewable Energy, Office of Energy Systems Research, Energy Storage Division of the U.S. Department of Energy under Contract Number DE-AC03-76SF00098

*Present address: Nikola Tesla, Telecommunication Equipment Factory, 41000 Zagreb, Moskovska 45, YUGOSLAVIA

INTRODUCTION

The zinc chlorine battery system is under development for load-leveling and electric vehicle applications. This secondary battery consists of a zinc electrode and a Cl_2 electrode in an aqueous solution of $ZnCl_2$ and KCl. During the charging process, Zn is deposited on the cathode and Cl_2 evolves on a porous flow-through graphite anode. The Cl_2 containing electrolyte flows into another chamber where it is chilled and stored in the form of solid chlorine hydrate ($Cl_2 \cdot 6H_2O$). During the discharge process zinc dissolves and the chlorine gas produced by heating the hydrate passes through the porous graphite electrode and forms chloride ions yielding aqueous $ZnCl_2$ [1]:

$$Zn + Cl_2(gas) = ZnCl_2(aqueous)$$

The cycle life, reliability, and coulombic efficiency of this battery depends on the quality of the zinc deposit. The macromorphology of the zinc deposit obtained from acidic $ZnCl_2$ solutions has been a subject of recent studies [1,5,8]. In this laboratory efforts have been concentrated on the evaluation of the effect of hydrodynamic flow on the macromorphology of zinc deposits. The influence of current density, pH, hydrodynamic conditions, deposition time, electrolyte composition, including impurities, have been examined. For the development of an understanding of the complex phenomena involved in zinc deposition, the mass transfer conditions near the electrode must be fully characterized.

The present work concerns the determination of limiting currents of zinc deposition from acidic $ZnCl_2$ and $ZnSO_4$ solutions. A rotating disk electrode has been used for this purpose.

For simple laminar flow at a rotating disk electrode, the dependence of mass transfer rate on relevant proven variables is expressed in the dimensionless equation:

$$Sh = 0.62\ Re^{1/2}\ Sc^{1/3} \qquad [1]$$

for $Re < 2.7 \times 10^5$

where $Sh = rk/D$

$Sc = \nu/D$

$Re = r^2\ \Omega/\nu$

$k = i_L/nFC_b$, mass transfer coefficient, cm/sec

This equation is the dimensionless form of Levich's rotating disk limiting current equation [13]:

$$i_L = 0.62\ n\ F\ D^{2/3}\ \Omega^{1/2}\ \nu^{-1/6}\ C_b \qquad [2]$$

ν = kinematic viscosity, cm^2/sec

Ω = angular velocity, rad/sec

r = disk radius, cm

c_b = bulk concentration of the reacting species, $moles/cm^3$

EXPERIMENTAL

Experimental Setup

The solutions were prepared from Analytical Reagent (AR) grade $ZnCl_2$, $ZnSO_4$, KCl, and Na_2SO_4 manufactured by Mallinckrodt. The rotating disk electrodes were made of 99.99% zinc. The 1.0 cm diameter zinc disk was attached to a brass core using silver-epoxy adhesive. The brass core was tapped on one end to screw onto the spindle shaft of the rotating disk assembly. Epoxy resin was cast around this brass core and zinc disk. The RDE was then machined to cylindrical shape, with a final outer diameter of 3.5 cm (Figures 1a and 1b). A one-compartment electrolyte cell with a 99.99% zinc circular anode located at the bottom of the cell was used in this investigation. This same cell (Figures 2a and 2b) was used in the previous investigations by Jaksic and Komnenic. The reference electrode was a saturated calomel electrode. Ohmic resistance was minimized by locating the Luggin capillary as close as possible to the disk in the plane of the disk, 3-4 cm from its center. The zinc disk study was carried out under potentiostatic control; the circuit diagram is shown in Figure 3a. Potentiostat-galvanostat, Princeton Applied Research Co. (PAR) Model 371, with a PAR Model 178 Electrometer Probe and PAR Model 175 Universal Programmer were used in the potentiostatic experiments. The rotator was a Pines Instrument ASR-2 rotator. Cathodic polarization curves were recorded on a Hewlett-Packard Model 7001A X-Y recorder (Figure 3b).

Experimental Procedure

The pretreatment of the zinc disk electrode was as follows:

a) polishing with waterproof SiC paper, (grit size 400, followed by 600)

b) polish with 1 micron-size diamond paste

c) washing with soap, rinsing with ethyl alcohol and acetone

d) before the experiment, dipping for 1 second in conc HNO3, and then rinsing with distilled water

Cathodic polarization of the zinc RDE was carried out in five different solutions:

0.05 M $ZnCl_2$ + 1 M KCl

0.10 M $ZnCl_2$ + 1 M KCl

0.50 M $ZnCl_2$ + 1 M KCl

0.05 M $ZnSO_4$ + 1 M Na_2SO_4

0.10 M $ZnSO_4$ + 1 M Na_2SO_4

The following six rotational speeds were used in this study: 200, 400, 800, 1200, 1600, 2000 revolutions per minute (rpm). The polarization curves were obtained by sweeping the potential range, -1.050 V to -2.550 V vs. SCE at scan rates of 10, 100, and 200 mV/s.

Half-cell reactions were:

$Zn^{+2} + 2e^- = Zn$ Eo = -0.763 V (working cathode)

$2Hg + 2\,Cl^- = Hg_2Cl_2 + 2e^-$ Eo = +0.242 V (reference electrode)

The viscosity of the solutions was measured with a Cannon-Fenske viscosimeter [4].

RESULTS

Cathodic polarization curves were obtained with the zinc disk at different rotational speeds, different concentrations of $ZnCl_2$ and $ZnSO_4$ solutions and using 3 different potential sweep rates. Each cathodic polarization curve was obtained with a freshly polished electrode surface. Supporting electrolyte was used to minimize potential variations in the solution and to keep the concentration of zinc at a low level in order to prevent large limiting currents. Zinc is highly complexed in chloride solutions even at the 0.05 M zinc concentrations used in these experiments [9,14]. The measured limiting current in chloride solution is actually a net quantity resulting from zinc transport by convective diffusion to the electrode and from additive or subtractive migrational contributions of the zinc ionic species.

Rotating Disk Studies in $ZnCl_2$ + KCl Solutions

Figure 4 shows the polarization curves at a scan rate of 10 mV/sec, in 0.05 M $ZnCl_2$ + 1 M KCl solution, pH = 2.48, T = 22°C. At all rotational speeds a well defined limiting current plateau was reached within the potential sweep. The steep rise in the current which appears at about -1.870 V vs. SCE is due to hydrogen evolution. Hydrogen bubbles could be observed near the electrode surface after this potential was reached. This potential is in good agreement with a result reported by Kim and Jorne in 0.05 M $ZnCl_2$ solution [5]. The zinc reaction is diffusion controlled; the current is proportional to the square root of the rotational speed in good agreement with Levich theory [2], as shown in Figure 5. This can be seen from the plot of the current vs. square root of the rotational speed under a fixed potential on the limiting current plateau, E = -1.746 V vs. SCE. At higher rotational speeds (1600 and 2000 rpm) accurate limiting current plateaus could not be obtained. Increase in surface area due to surface roughening is the most probable explanation for this behavior [6].

After sweeping the potential at 10 mV/sec to just above the limiting current plateau, evidenced by the onset of hydrogen evolution, the electrodes were removed, washed, and dried, and Scanning Electron Microscopy (SEM) images of the zinc deposits were taken for the various rotational speeds. At the three lower rotational speeds (Figures 6, 7, 8) the dendritic growth covers the entire surface. The dendrites seen in these Figures are whiskery in shape and extend normal from the surface into the bulk solution. At the higher rotational speeds the dendritic growth was observed only near the disk edge (Figures 9, 10, 11) and was of layered and spiral form. This behavior is due to the secondary current distribution becoming more nonuniform at higher rotational speeds below the limiting current. At the same fraction of limiting current, the current density near the disk edge is higher at higher rpms, and the surface near the edge becomes more rough. At limiting current the current distribution is uniform over the electrode, but a dendritic zinc deposit with a high surface area has already been formed.

Substantial surface roughening can prevent obtaining a limiting current plateau because the surface area increases during the measurement, causing a corresponding increase in limiting current [6]. In order to avoid the rapid development of surface roughness during measurement, higher potential scan rates were used. The results for a high scan rate of 200 mV/sec is shown in Figure 12 for 0.05 M $ZnCl_2$ + 1 M

KCl. Accurate limiting current plateaus at the higher rotational speeds were obtained using these higher scan rates. The diffusion coefficent for Zn^{+2} was calculated from the limiting currents obtained in Figures 5 and 12, and is tabulated in Table 1. At the lower potential scan rate, 10 mV/sec, the calculated diffusion coefficient for Zn^{+2} is lower than literature values (Table 3), but the experimental result at the higher scan rates is in good agreement with values of Zn^{+2} diffusion coefficients reported previously [5,7]. The zinc deposition is shown to be diffusion controlled and the limiting current is proportional to the square root of the rotational speed for the higher scan rates in Figure 13. Using 200 mV/sec scan rate data, the average diffusion coefficient for Zn^{+2} at 22°C in 0.05 M $ZnCl_2$ + 1 M KCl is $D = 0.981 \pm 0.050 \times 10^{-5}$ cm^2/sec.

Numerous experiments in 0.10 M $ZnCl^2$ + 1 M KCl at various rotational speeds and potential sweep rates were made in order to study the effect of concentration on the diffusion coefficient of Zn^{+2}. Results are shown in Figure 14. Accurate limiting current plateaus were obtained only at the potential scan rate of 200 mV/sec. At the higher rotational speeds, the current becomes independent of the rotational speed and the zinc electrodeposition reaction is no longer diffusion controlled (Figure 13). The average diffusion coefficient for Zn^{+2} in 0.10 M $ZnCl_2$ + 1 M KCl at 22°C is $D = 0.892 \pm 0.067 \times 10^{-5}$ cm^2/sec. Experimental data are summarized in Table 1. The experimental results show that more accurate limiting current plateaus for the higher rotational speeds and scan rates can be obtained at lower zinc concentrations.

In 0.50 M $ZnCl_2$ + 1 M KCl solution a limiting current plateau could only be obtained with 200 and 400 rpm and at the highest scan rate, 200 mV/sec (Figure 15). The average diffusion coefficient obtained was 0.583×10^{-5} cm^2/sec. At higher rotational speeds and lower sweep rates limiting current plateaus were not discernible.

<u>Rotating Disk Studies in $ZnSO_4$ + Na_2SO_4 Solutions</u>

In acidic chloride solutions, zinc forms various chloride complexes in addition to the simple cation: $ZnCl_4^{--}$, $ZnCl_3^-$, $ZnCl_2$, $ZnCl^+$ [9,14]. In order to demonstrate the influence of zinc chloride complexes in the foregoing limiting current measurements, experiments in acidic $ZnSO_4$ + Na_2SO_4 solutions were also performed. No reference to sulfate complexes of zinc were found in the literature [9].

Figure 16 shows the polarization curves at scan rate 200 mV/sec in 0.05 M $ZnSO_4$ + 1 M Na_2SO_4, pH = 2.39, T = 22°C. Zinc deposition limiting current plateaus were obtained at various rotational speeds. The results are similar to results shown in Figure 12 for the chloride solution except that the potentials at which hydrogen starts to evolve predominantly is shifted to more negative values in the sulfate solution compared to the chloride solution.

The plot of current vs. square root of the rotational speed is shown in Figure 17 at a fixed potential on the limiting current plateau E = -2.300 V vs. SCE. The zinc deposition reaction is diffusion controlled and the average diffusion coefficient for Zn^{+2} at 22°C in 0.05 M $ZnSO_4$ + 1 M Na_2SO_4 is $D = 0.786 \pm 0.038 \times 10^{-5}$ cm^2/sec.

Several experiments were performed in 0.10 M $ZnSO_4$ + 1 M Na_2SO_4, pH = 2.5, T = 22°C at various rotational speeds. Figure 18 shows the polarization curves at a scan rate of 200 mV/sec. At the higher rpms, accurate limiting current plateaus could not be obtained, just as in the chloride system.

From Figure 17, at E = -2.404 V vs. SCE, it can be seen that the current at higher rpms is still proportional to the square root of the rotational speed, thus the reaction is diffusion controlled. The average diffusion coefficient for Zn^{+2} at 22°C in 0.10 M $ZnSO_4$ + 1 M Na_2SO_4 is $D = 0.565 \pm 0.023 \times 10^{-5}$ cm^2/sec. The zinc sulfate experimental data are summarized in Table 2.

DISCUSSION

The experimental diffusivity data show slightly higher values of the zinc diffusion coefficient in 0.05 M $ZnSO_4$ than in 0.05 M $ZnCl_2$, and show a dependence upon both the rotational speed and sweep rate. The average diffusion coefficient decreases as the concentration of zinc increases. Experiments with higher zinc concentrations were attempted, but limiting current plateaus could not be obtained. The higher currents needed in more concentrated solutions caused even more rapid increase in the surface area of the zinc deposit.

The diffusion coefficients obtained in this study are compared with other available diffusion data in Table 3. Substantial differences exist between the diffusion coefficients reported for $ZnCl_2$ solutions by the interferometric measurements and those obtained by electrochemical measurements. These differences arise from the diffusional quantities measured by the two experimental techniques. The interferometric methods use a free-diffusion, stagnant cell to measure zinc diffusivities, while the electrochemical methods yield effective diffusion coefficients under forced-convection conditions. The formation of zinc-chloro-complex ions may also influence the two types of diffusion coefficients to different degrees in the $ZnCl_2$ solutions. Miller and Rard [10,15] also present component diffusion coefficients for the ternary ($ZnCl_2$-KCl-H_2O) system.

The $ZnSO_4$ results are more ambiguous in that they show a large decrease in the diffusion coefficient with increasing concentration. Surface roughening arguments cannot justify such a large decline in diffusion coefficient. The results by Albright and Miller [11] show a similar but smaller dependence on concentration than this work; the authors suggest that the decline is due to ion-pair formation, which causes greater structuring in more concentrated solutions.

SUMMARY

Mass transfer limiting currents in acidic $ZnCl_2$ and $ZnSO_4$ solutions were investigated. Cathodic polarization curves were obtained by potential scans at various rotational speeds of a zinc disk electrode. The surface roughness of zinc during slow potential scan rates (10 mV/sec) and high rotational speeds (1600,2000 rpm) prevented obtaining limiting current plateaus. However, at higher scan rates, distinct limiting current plateaus were defined. From the limiting current, the diffusion coefficient was calculated, $D = 0.98 \pm 0.05 \times 10^{-5}$ cm^2/sec (0.05 M $ZnCl_2$ + 1 M KCl). In 0.10 $ZnCl_2$ + 1 M KCl at the higher rotational speeds a limiting current plateau could not be observed at the higher potential scan rates. Experiments in acidic $ZnSO_4$ solution showed similar results. The zinc diffusion coefficient obtained from these experiments was $D = 0.78 \pm 0.04 \times 10^{-5}$ cm^2/sec (0.05 M $ZnSO_4$ + 1 M Na_2SO_4).

ACKNOWLEDGEMENT

This work was supported by the Assistant Secretary for Conservation and Renewable Energy, Office of Energy Systems Research, Energy Storage Division of the U.S. Department of Energy under Contract Number DE-AC03-76SF00098.

REFERENCES

1. J. Jorne, J. T. Kim, and D. Kralik, J. Appl. Electrochem., 9 (1979), p. 573.

2. J. Newman, Electrochemical Systems, Prentice-Hall, Inc., Englewood Cliffs, NJ, (1973).

3. J. Newman, JES, 113 (1966), p. 501.

4. J. R. Van Wazer, Viscosity and Flow Measurement, Interscience Publishers, NY, (1963).

5. J. T. Kim and J. Jorne, JES, 127 (1980), p. 8.

6. N. Ibl and K. Schadegg, JES, 114 (1967), p. 54.

7. D. Loftus, J. Roberts, R. Weaver, S. Leach and L. Nanis, "Diffusivity in $ZnCl_2$-KCl Electrolyte", Stanford Research Institute, International, EPRI Project Final Report, January 15, 1982.

8. U. Landau, B. Cahan, and J. Selman, EPRI Project #1198-3, Final Report, September 1978 - November 1980.

9. L. Sillen, ed., Stability Constants of Metal Ion Complexes, The Chemical Society, London, (1964).

10. D. Miller and J. Rard, "Transport in Aqueous Battery Systems", Lawrence Livermore National Laboratory, Contract Final Report, December 31, 1981.

11. J. Albright and D. Miller, J. Solution Chemistry, 4 (1975), p. 809.

12. A. Agnew and R. Patterson, Faraday Transactions I, 74 (1978), p. 2896.

13. Veniamin G. Levich, Physicochemical Hydrodynamics, Prentice-Hall, Inc., Englewood Cliffs, NJ, (1962).

14. James McBreen and Elton J. Cairns, "The Zinc Electrode", in Advances in Electrochemistry and Electrochemical Engineering, Vol. 11, H. Gerischer and C. W. Tobias, eds., Interscience, New York (1977).

15. D. Miller and J. Rard, "Transport in Aqueous Battery Systems", Lawrence Livermore National Laboratory, Contract Report for October 1 - December 31, 1982.

Table 1. Experimental Data and Results for Deposition of Zinc from $ZnCl_2$ + 1 M KCl Solution

Expt.	$ZnCl_2$ Conc. M	i_L mA/cm^2	k x10^{-3} cm/sec	D x10^{-5} cm^2/sec	Ω rpm	Sweep Rate mV/sec	ν x10^{-2} cm^2/sec	Sc	Re
1	0.05	15.3	1.6	0.419	200	10	0.9969	2380	525
2	0.05	12.9	1.3	0.324	200	10	0.9969	3080	525
3	0.05	20.2	2.1	0.376	400	10	0.9969	2650	1050
4	0.05	20.9	2.2	0.399	400	10	0.9969	2500	1050
5	0.05	28.2	2.9	0.371	800	10	0.9969	2690	2100
6	0.05	26.6	2.8	0.339	800	10	0.9969	2940	2100
7	0.05	34.6	3.6	0.372	1200	10	0.9969	2680	3150
8	0.05	33.0	3.4	0.347	1200	10	0.9969	2870	3150
9	0.05	41.3	4.3	0.388	1600	10	0.9969	2570	4200
10	0.05	37.9	3.9	0.343	1600	10	0.9969	2910	4200
11	0.05	44.3	4.6	0.367	2000	10	0.9969	2720	5250
12	0.05	41.9	4.3	0.337	2000	10	0.9969	2960	5250
13	0.05	25.8	2.7	0.916	200	100	0.9969	1090	525
14	0.05	22.5	2.3	0.746	200	100	0.9969	1340	525
15	0.05	24.2	2.5	0.832	200	100	0.9969	1220	525
16	0.05	26.8	2.8	0.966	200	200	0.9969	1030	525
17	0.05	28.0	2.9	1.032	200	200	0.9969	970	525
18	0.05	38.2	4.0	0.980	400	200	0.9969	1020	1050
19	0.05	40.8	4.3	1.081	400	200	0.9969	920	1050
20	0.05	53.5	5.5	0.965	800	200	0.9969	1030	2100
21	0.05	53.5	5.5	0.965	800	200	0.9969	1030	2100
22	0.05	65.0	6.7	0.953	1200	200	0.9969	1050	3150
23	0.05	63.7	6.6	0.925	1200	200	0.9969	1080	3150
24	0.05	80.3	8.3	1.055	1600	200	0.9969	940	4200
25	0.05	73.9	7.7	0.932	1600	200	0.9969	1070	4200
26	0.05	85.4	8.8	0.979	2000	200	0.9969	1020	5250
27	0.05	82.8	8.6	0.935	2000	200	0.9969	1070	5250
28	0.10	48.4	2.5	0.846	200	200	1.011	1200	518
29	0.10	53.5	2.8	0.983	200	200	1.011	1030	518
30	0.10	79.0	4.1	1.033	400	200	1.011	980	1036
31	0.10	70.1	3.6	0.878	400	200	1.011	1150	1036
32	0.10	98.1	5.1	0.850	800	200	1.011	1190	2072
33	0.10	98.1	5.1	0.850	800	200	1.011	1190	2072
34	0.10	118.5	6.1	0.832	1200	200	1.011	1220	3108
36	0.10	124.8	6.5	0.914	1200	200	1.011	1110	3108
37	0.10	137.6	7.1	0.854	1600	200	1.011	1180	4144
38	0.10	99.1	5.1	0.877	800	100	1.011	1150	2072
39	0.50	191.0	2.0	0.593	200	200	1.080	1820	485
40	0.50	188.0	1.9	0.580	200	200	1.080	1860	485
41	0.50	188.0	1.9	0.580	200	200	1.080	1860	485
42	0.50	265.0	2.7	0.577	400	200	1.080	1870	970
43	0.50	268.0	2.8	0.584	400	200	1.080	1850	970

Table 2. Experimental Data and Results for Deposition of Zinc from $ZnSO_4$ + 1 M Na_2SO_4 Solution

Expt.	$ZnSO_4$ Conc. M	i_L mA/cm^2	k x10^{-3} cm/sec	D x10^{-5} cm^2/sec	Ω rpm	Sweep Rate mV/sec	ν x10^{-2} cm^2/sec	Sc	Re
1	0.05	24.2	2.5	0.852	200	100	1.112	1310	471
2	0.05	22.9	2.4	0.785	200	200	1.112	1420	471
3	0.05	34.4	3.6	0.860	400	100	1.112	1290	942
4	0.05	31.8	3.3	0.765	400	100	1.112	1450	942
5	0.05	31.8	3.3	0.765	400	200	1.112	1450	942
6	0.05	45.9	4.8	0.788	800	100	1.112	1410	1884
7	0.05	45.9	4.8	0.788	800	100	1.112	1410	1884
8	0.05	44.6	4.6	0.755	800	200	1.112	1470	1884
9	0.05	54.8	5.7	0.758	1200	100	1.112	1470	2826
10	0.05	54.8	5.7	0.758	1200	200	1.112	1470	2826
11	0.05	67.5	7.0	0.836	1600	100	1.112	1330	3768
12	0.05	66.2	6.9	0.812	1600	100	1.112	1370	3768
13	0.05	63.7	6.6	0.766	1600	200	1.112	1450	3768
14	0.05	71.3	7.4	0.768	2000	100	1.112	1450	4710
15	0.05	68.8	7.1	0.728	2000	100	1.112	1530	4710
16	0.10	36.9	1.9	0.569	200	200	1.118	1960	468
17	0.10	36.9	1.9	0.569	200	200	1.118	1960	468
18	0.10	34.4	1.8	0.512	200	100	1.118	2180	468
19	0.10	53.5	2.8	0.590	400	200	1.118	1890	936
20	0.10	53.5	2.8	0.590	400	200	1.118	1890	936
21	0.10	53.5	2.8	0.590	400	200	1.118	1890	936
22	0.10	73.9	3.8	0.570	800	200	1.118	1960	1872
23	0.10	75.2	3.9	0.585	800	200	1.118	1910	1872
24	0.10	71.3	3.7	0.540	800	200	1.118	2070	1872
25	0.10	89.2	4.6	0.558	1200	200	1.118	2000	2808
26	0.10	89.2	4.6	0.558	1200	200	1.118	2000	2808
27	0.10	89.2	4.6	0.558	1200	200	1.118	2000	2808
28	0.10	101.9	5.3	0.548	1600	200	1.118	2040	3744
29	0.10	103.2	5.3	0.599	1600	200	1.118	1870	3744
30	0.10	114.6	5.9	0.554	2000	200	1.118	2020	4680
31	0.10	114.6	5.9	0.554	2000	200	1.118	2020	4680

Table 3. Comparison of Diffusion Coefficients of Zinc with Literature Data

Reference	Solution	Method	Temp. (^oC)	pH	Concentrations (M) (D in 10^{-5} cm^2/sec)						
					0.05	0.1	0.2	0.4	0.5	1.0	1.6
Present Study	$ZnCl_2$ + 1 M KCl	RDE	22	2.4	0.98	0.89			0.58		
5	$ZnCl_2$ + 1 M KCl	RDE	25		0.89						
7	$ZnCl_2$ + 3.5 M KCl	Capillary	26.5					0.82			0.88
8	$ZnCl_2$ + 3 M KCl	Polarography	25	3.5		0.52			0.45	0.41	
10	$ZnCl_2$	Interferometry	25				1.027	1.007			
12	$ZnCl_2$	Interferometry	25		1.048						
15	$ZnCl_2$	Interferometry	25					1.003	0.991		
Present Study	$ZnSO_4$ + 1 M Na_2SO_4	RDE	22	2.5	0.78	0.57					
11	$ZnSO_4$	Interferometry	25		0.60	0.56	0.51		0.43	0.37	

FIGURE CAPTIONS

Fig. 1a. Rotating disc zinc electrode.

Fig. 1b. RDE electrolysis cell.

Fig. 2a. Cell for Zn-RDE studies.

Fig. 2b. Experimental apparatus.

Fig. 3a. Circuit for potentiostatic deposition of zinc.

Fig. 4. Limiting current plateaus in 0.05 M $ZnCl_2$ + 1 M KCl.

Fig. 5. Dependence of i_L on rpm (Levich plot).

Fig. 6. SEM micrographs of zinc deposits on RDE in 0.5 M $ZnCl_2$ + 1 M KCl, above the limiting current at rotation speed 200 rpm. Magnification: (A) 10x, (B) 500x, (C) original RDE surface before zinc deposition, 500x, (D) 2000x.

Fig. 7. SEM micrographs of zinc deposits on RDE in 0.05 M $ZnCl_2$ + 1 M KCl, above the limiting current at rotation speed 400 rpm. Magnification: (A) 10x, (B) 500x, (C) 2000x.

Fig. 8. SEM micrographs of zinc deposits on RDE in 0.05 M $ZnCl_2$ + 1 M KCl, above the limiting current at rotation speed 800 rpm. Magnification: (A) 10x, (B) 500x, (C) 2000x.

Fig. 9. SEM micrographs of zinc deposits on RDE in 0.05 M $ZnCl_2$ + 1 M KCl, above the limiting current at rotation speed 1200 rpm. Magnification: (A) 10x, (B) 500x, (C) 2000x.

Fig. 10. SEM micrographs of zinc deposits on RDE in 0.05 M $ZnCl_2$ + 1 M KCl, above the limiting current at rotation speed 1600 rpm. Magnification: (A) 10x, (B) 500x, (C) 2000x.

Fig. 11. SEM micrographs of zinc deposits on RDE in 0.05 M $ZnCl_2$ + 1 M KCl, above the limiting current at rotation speed 2000 rpm. Magnification: (A) 10x, (B) 500x, (C) 2000x.

Fig. 12. Limiting current plateaus in 0.05 M $ZnCl_2$ + 1 M KCl.

Fig. 13. Dependence of i_L on rpm (Levich plot).

Fig. 14. Limiting current plateaus in 0.10 M $ZnCl_2$ + 1 M KCl.

Fig. 15. Limiting current plateaus in 0.50 M $ZnCl_2$ + 1 M KCl.

Fig. 16. Limiting current plateaus in 0.05 $ZnSO_4$ + 1 M Na_2SO_4.

Fig. 17. Dependence of i_L on rpm (Levich plot).

Fig. 18. Limiting current plateaus in 0.10 $ZnSO_4$ + 1 M Na_2SO_4.

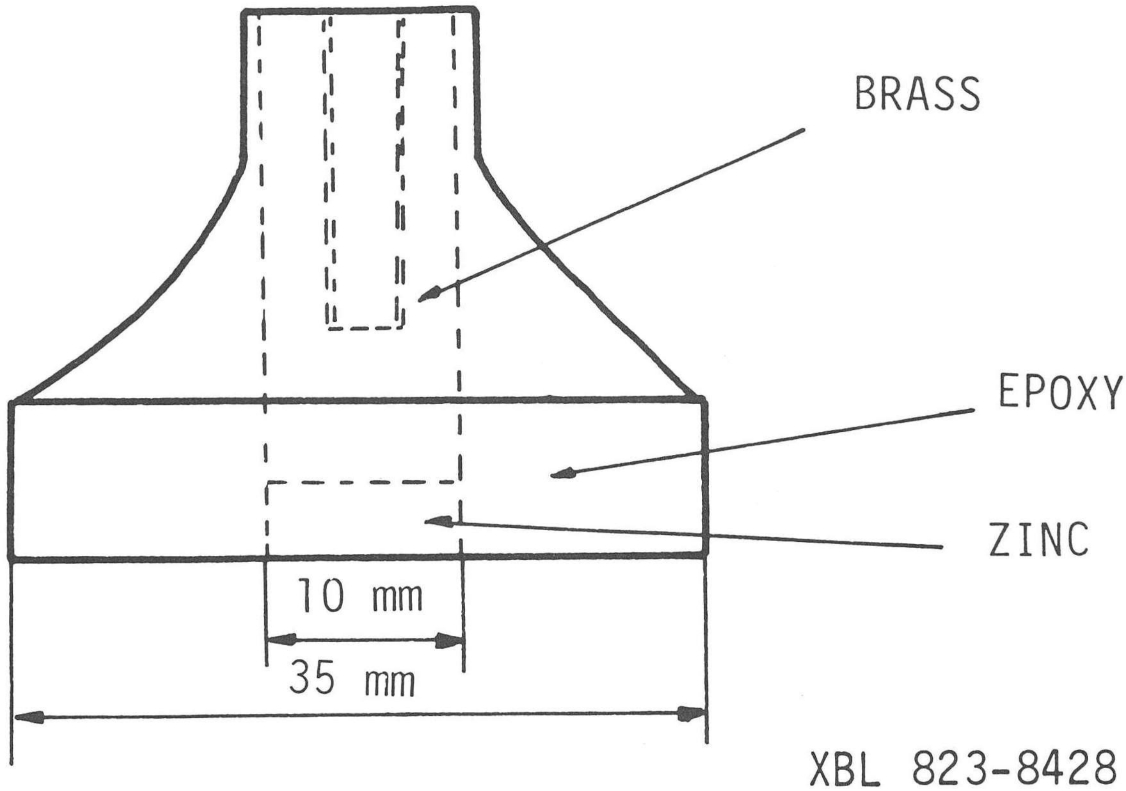

Fig. 1a

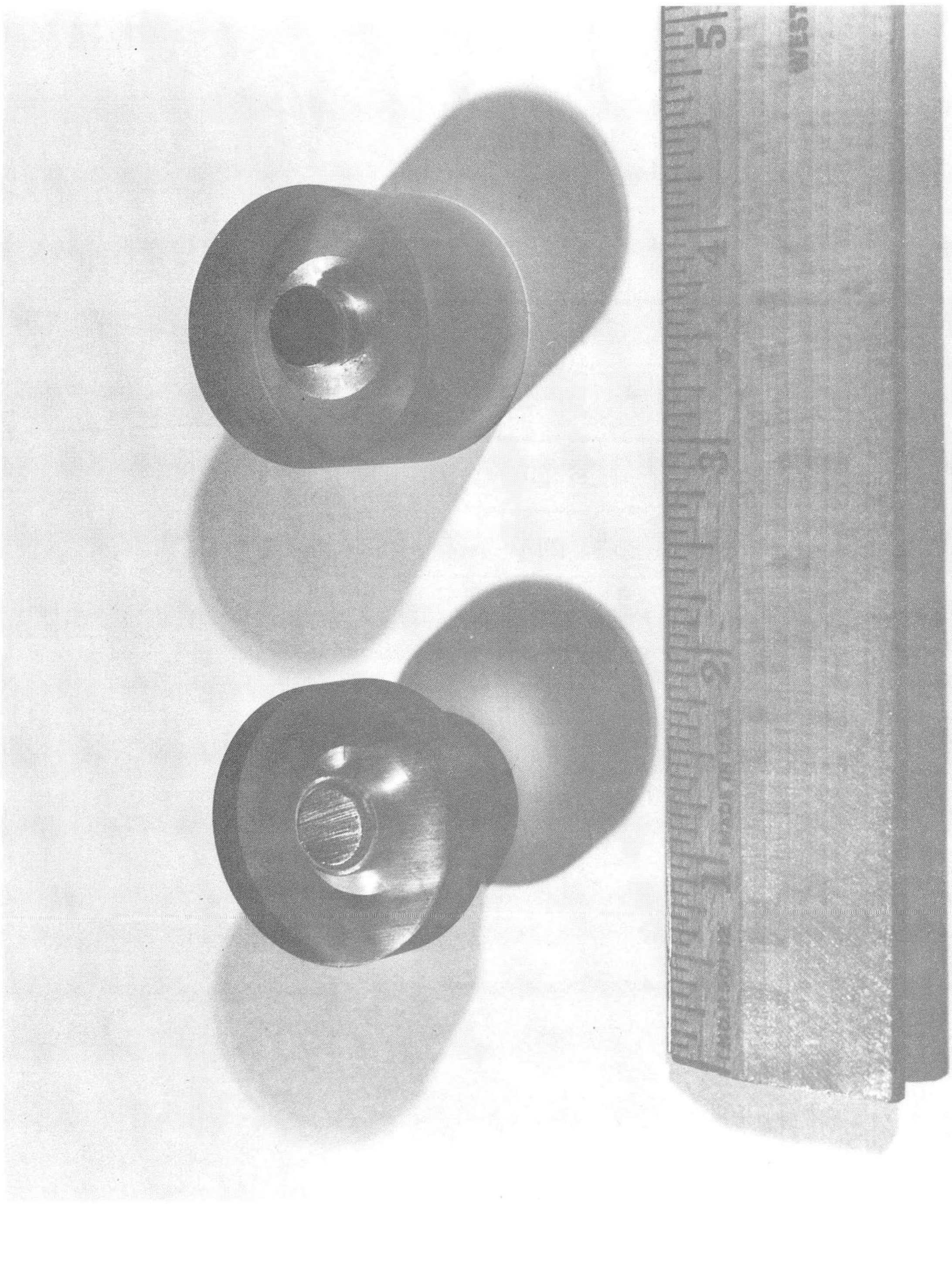

Fig. 1b

CBB 823-2852

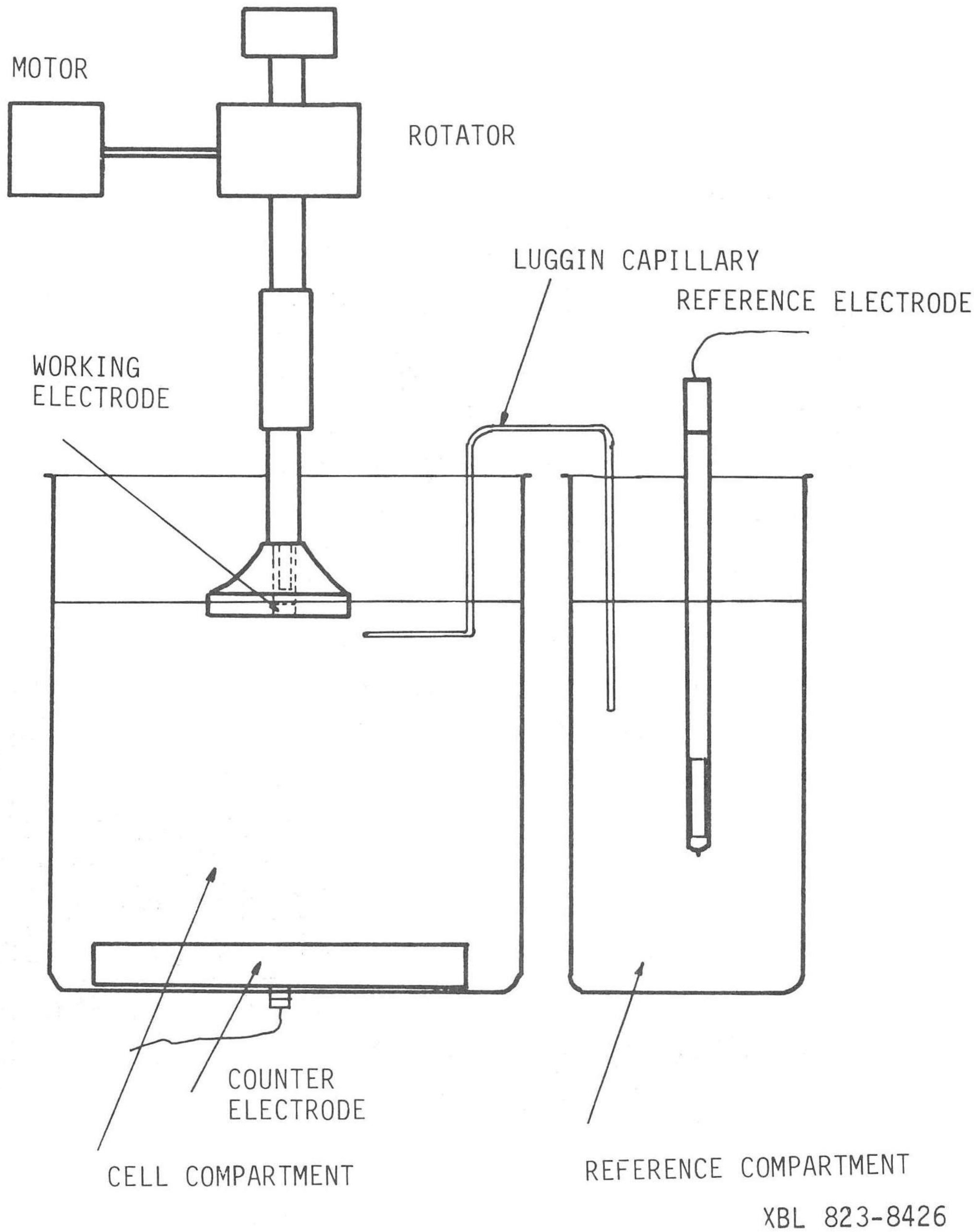
MOTOR
ROTATOR
LUGGIN CAPILLARY
REFERENCE ELECTRODE
WORKING
ELECTRODE
COUNTER
ELECTRODE
CELL COMPARTMENT
REFERENCE COMPARTMENT
XBL 823-8426

Fig. 2a.

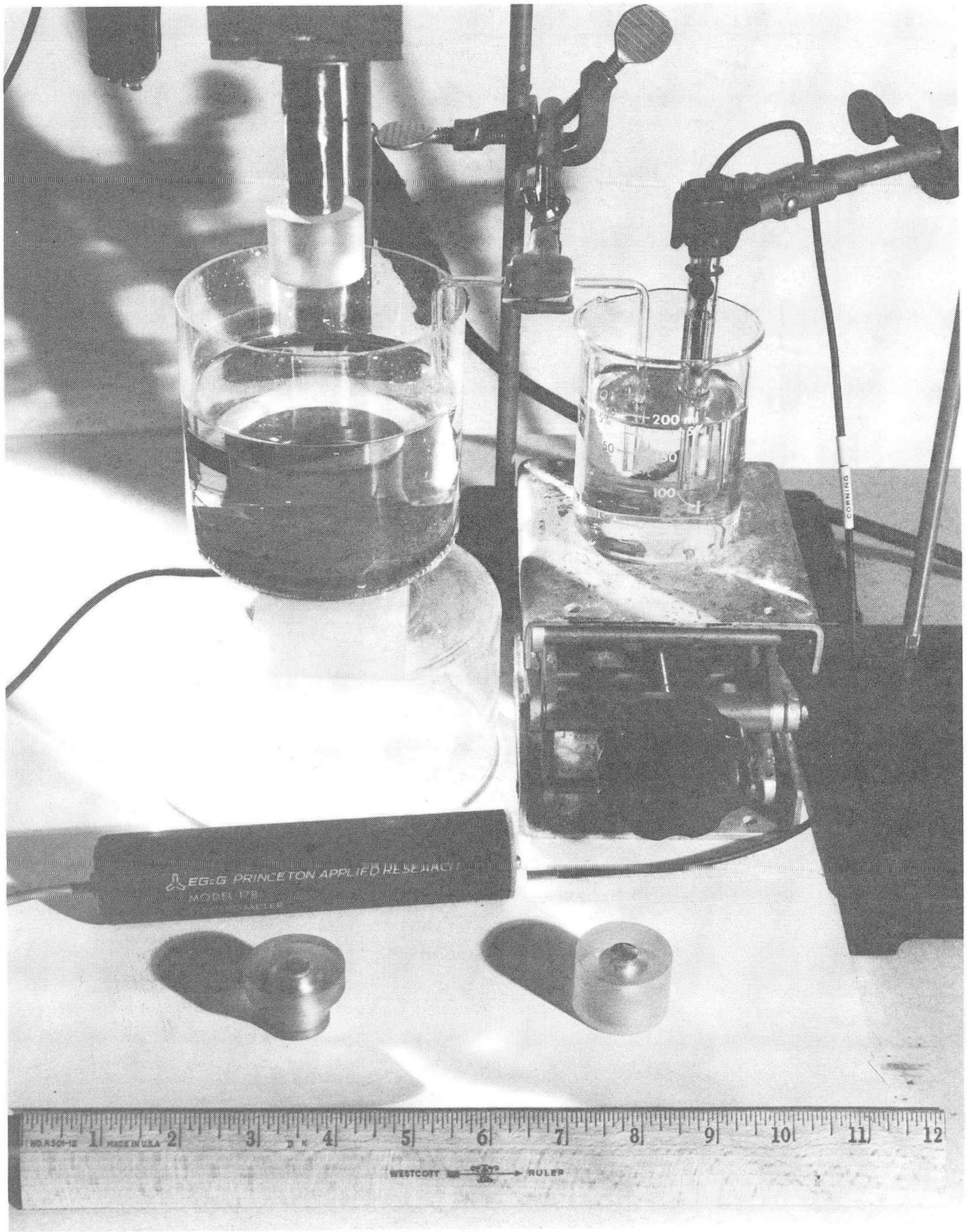

CBB 823-2854

Fig. 2b

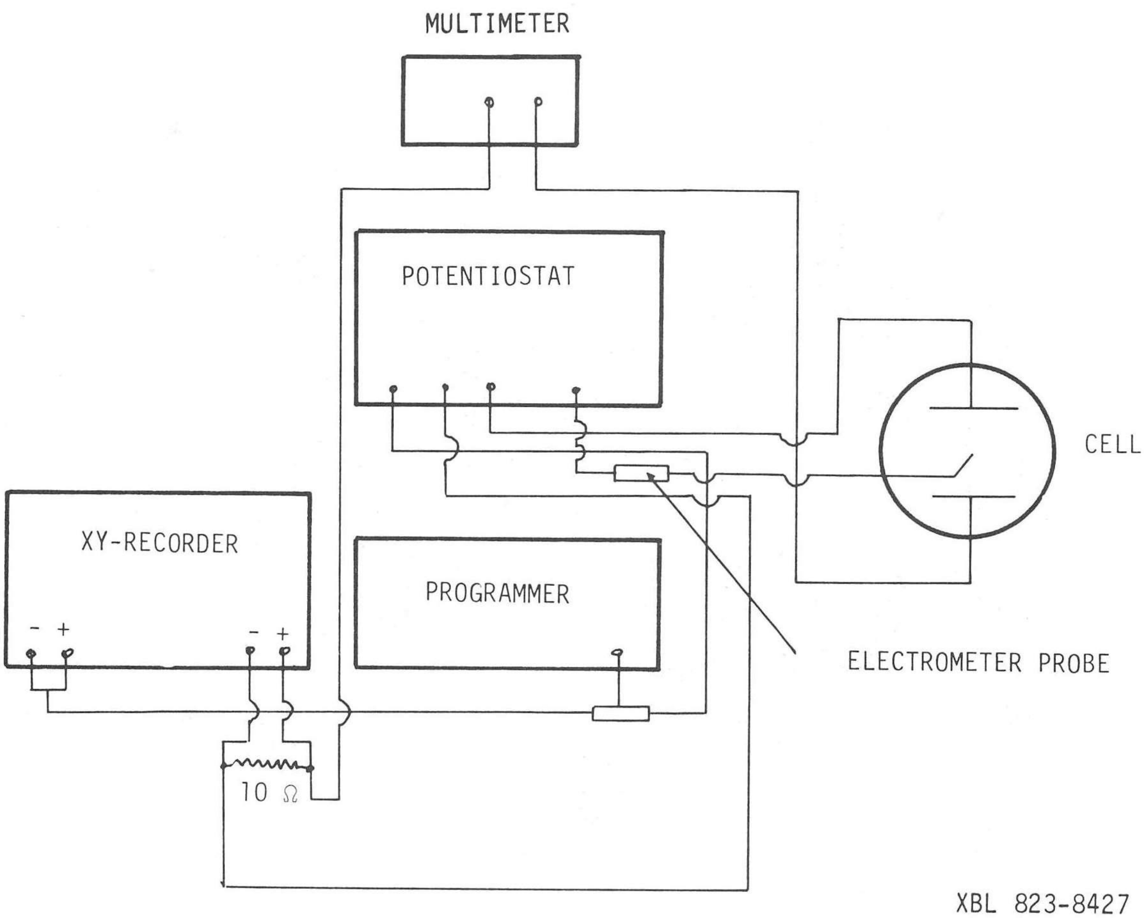
MULTIMETER
POTENTIOSTAT
CELL
XY-RECORDER
- +
- +
PROGRAMMER
ELECTROMETER PROBE
10 Ω
XBL 823-8427

Fig. 3a

Fig. 3b CBB 823-2850

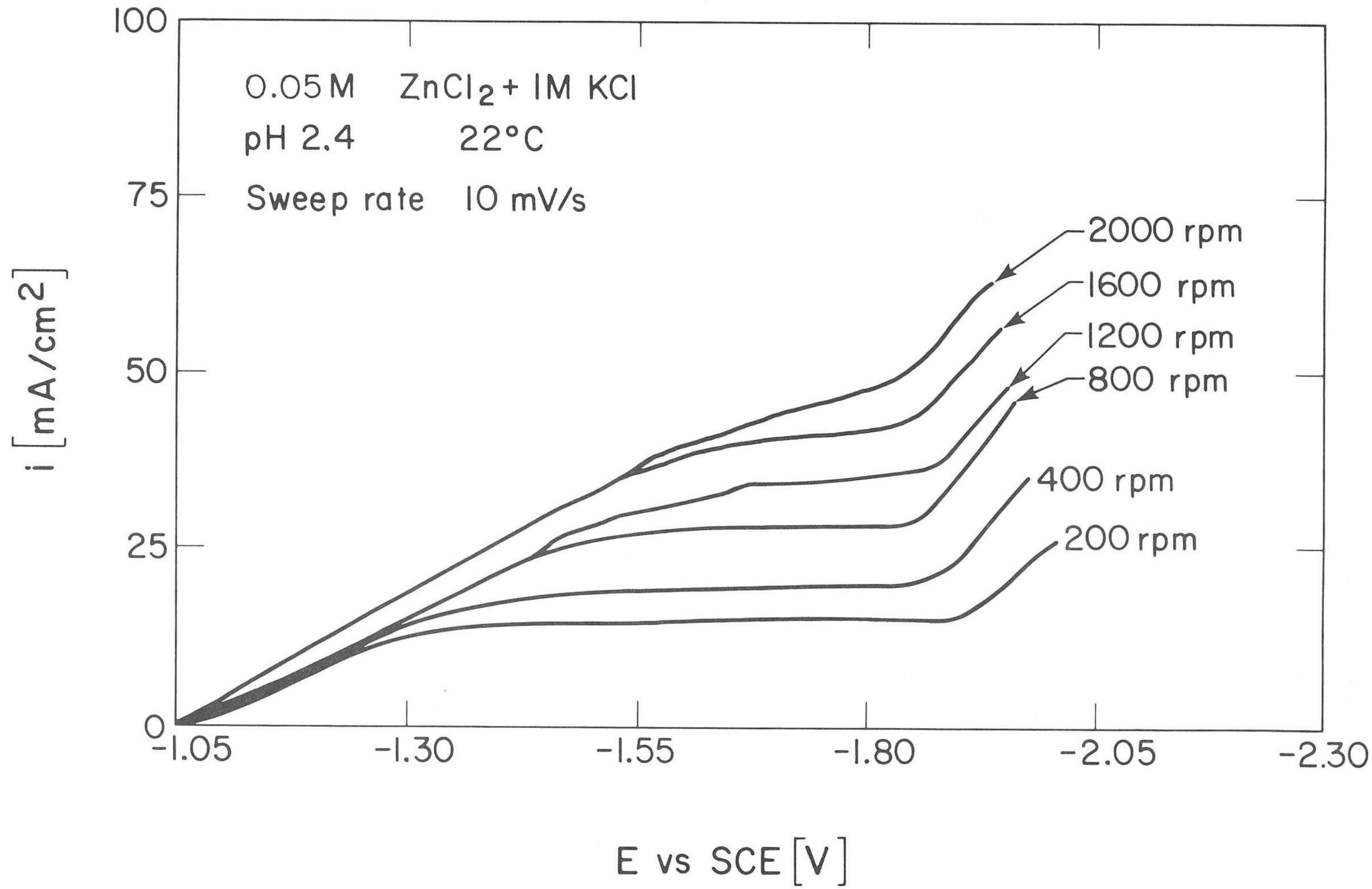

XBL 831-1052

Fig. 4

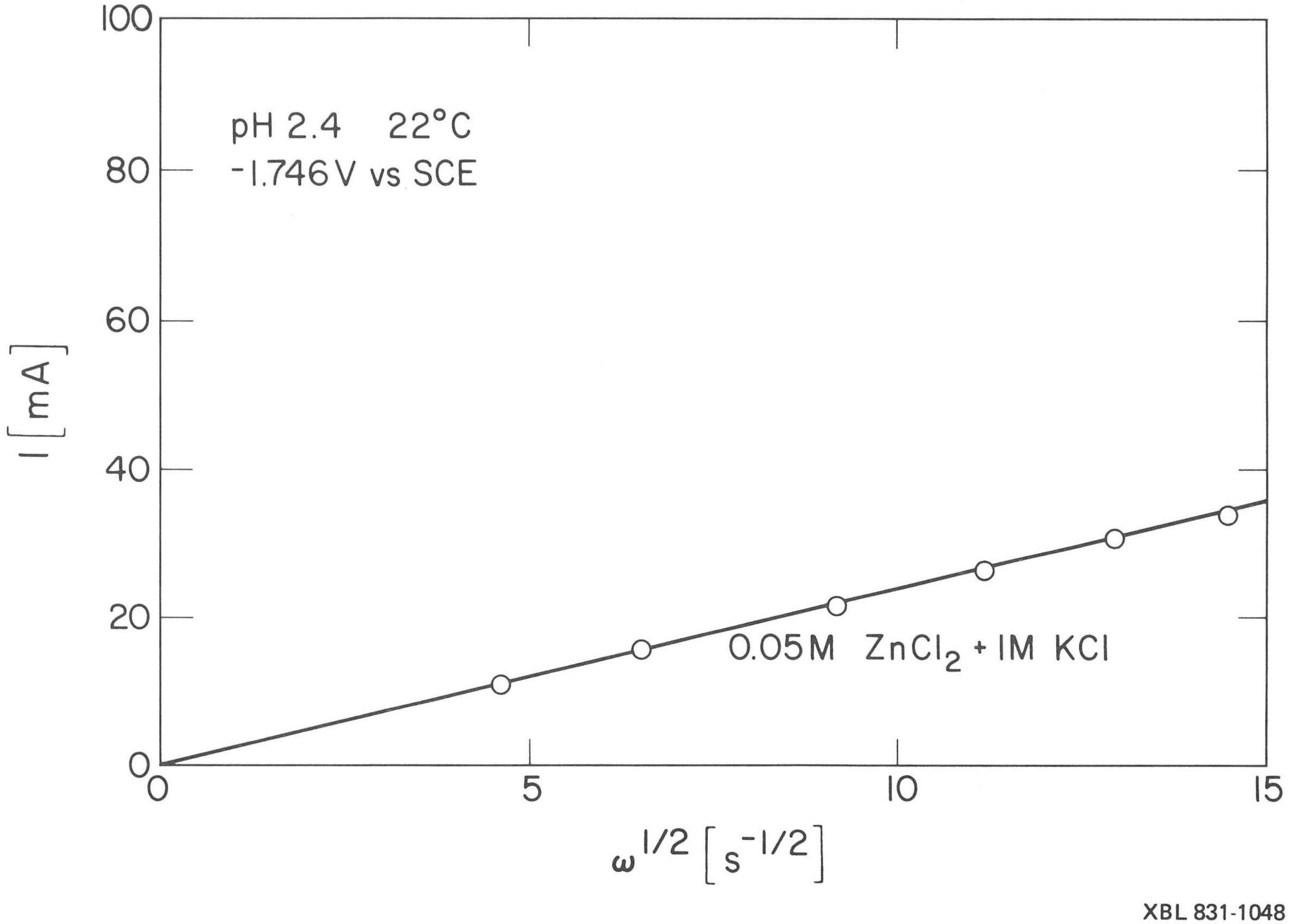
pH 2.4 22°C
-1.746 V vs SCE
0.05M ZnCl2 + 1M KCl
I [mA]
100
80
60
40
20
0
0
5
10
15
ω1/2 [s-1/2]
XBL 831-1048

Fig. 5

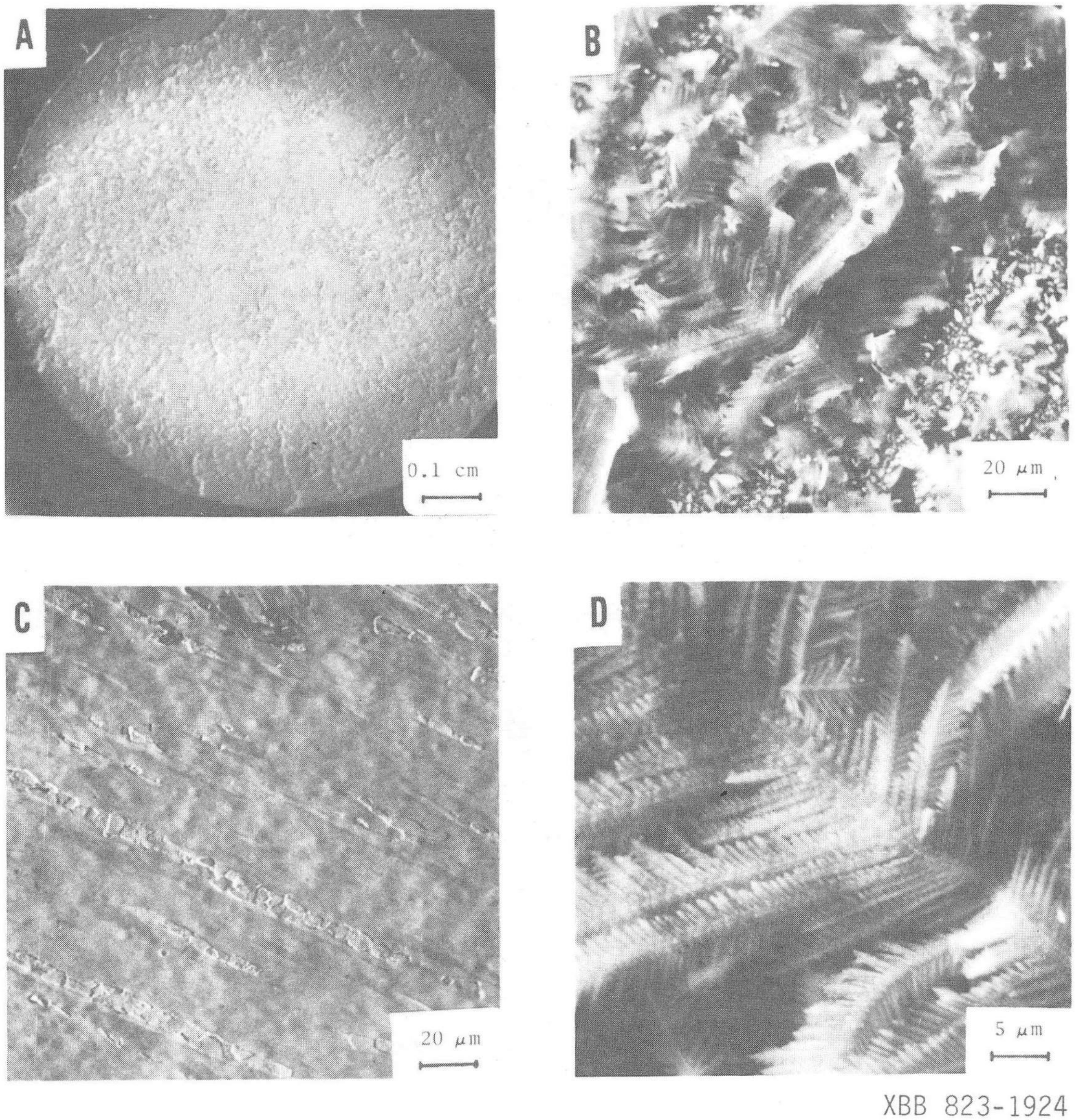

Fig. 6

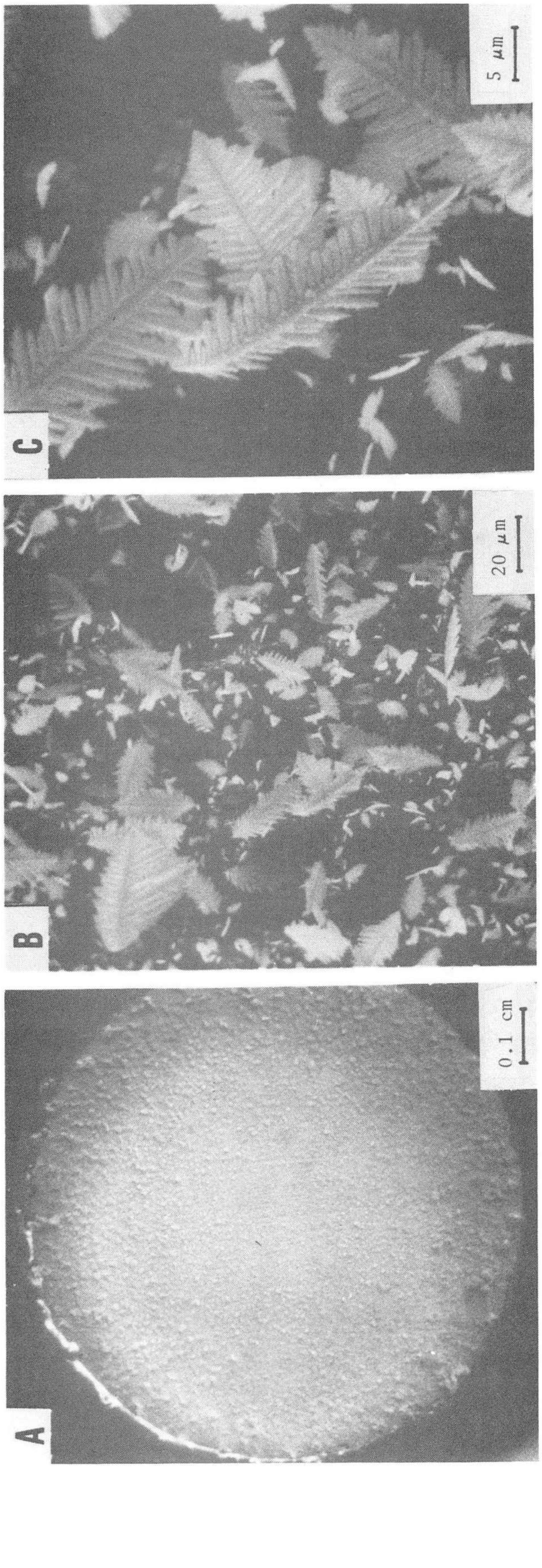

XBB 823-1925

Fig. 7

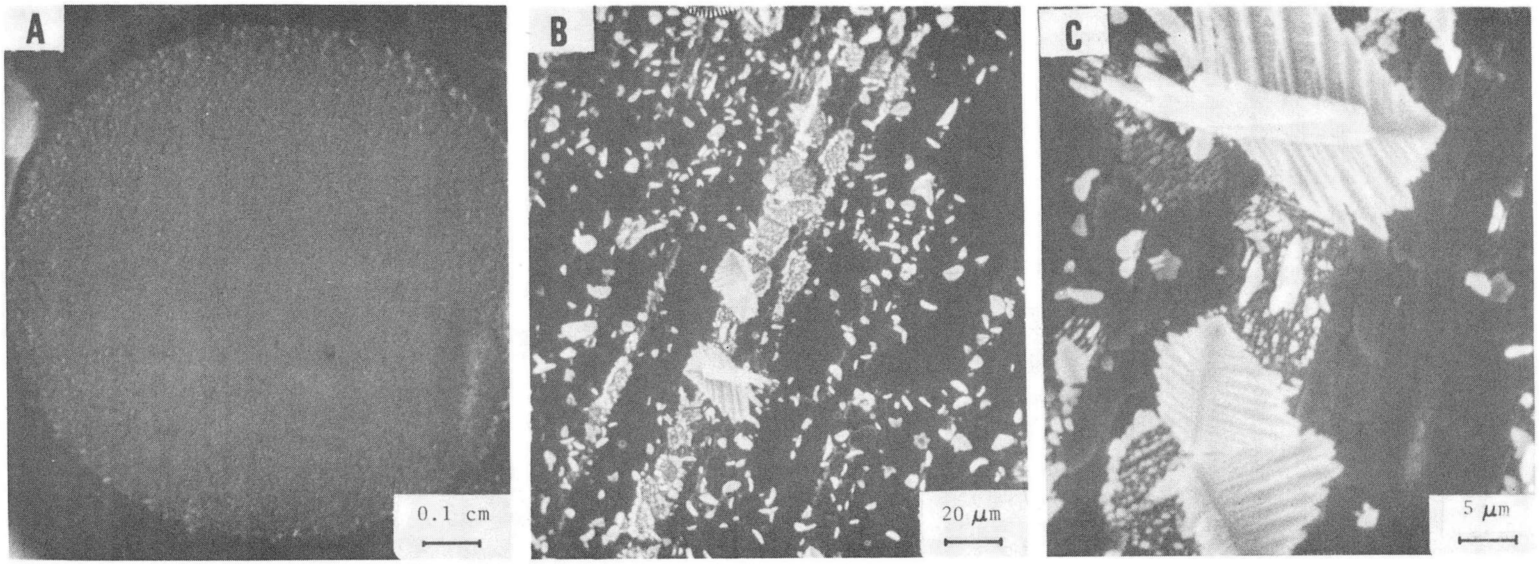

XBB 823-1926

Fig. 8

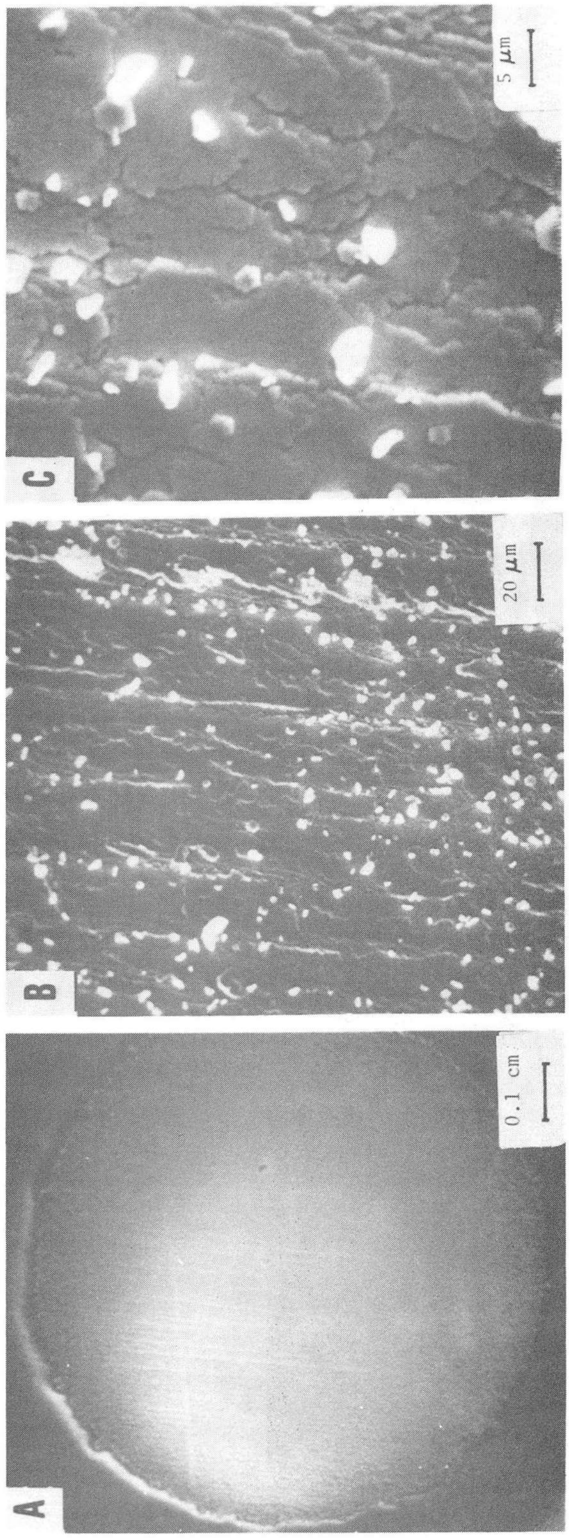

XBB 823-1927

Fig. 9

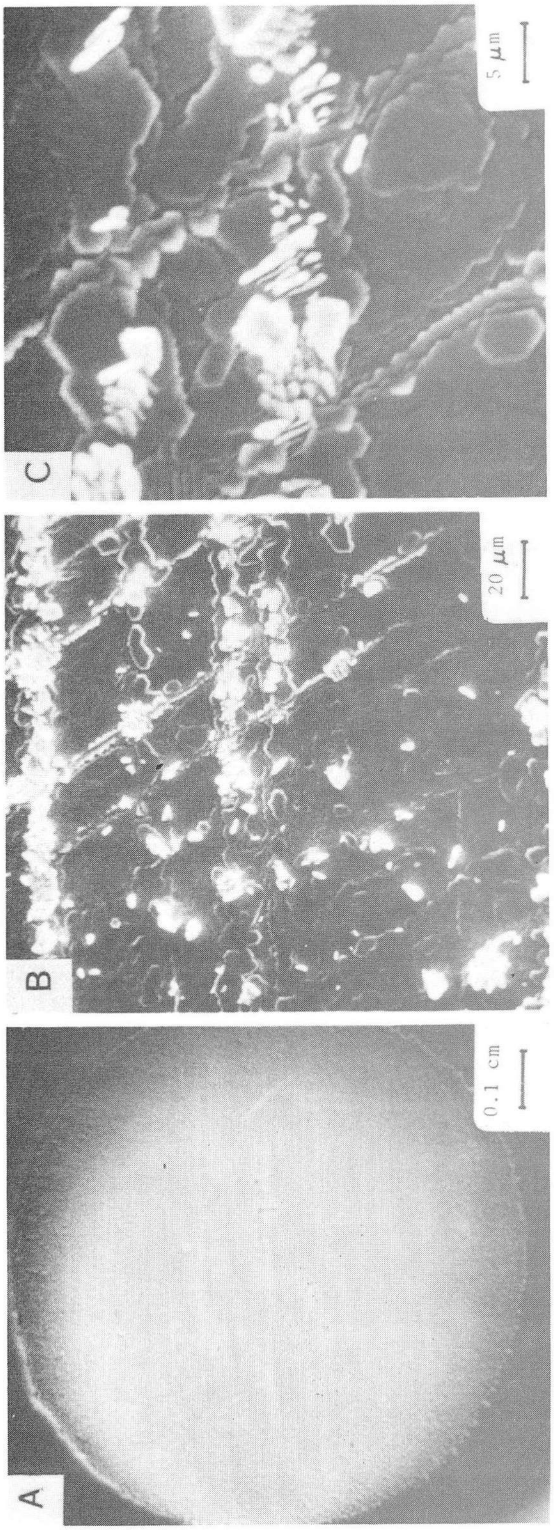

XBB 823-1928

Fig. 10

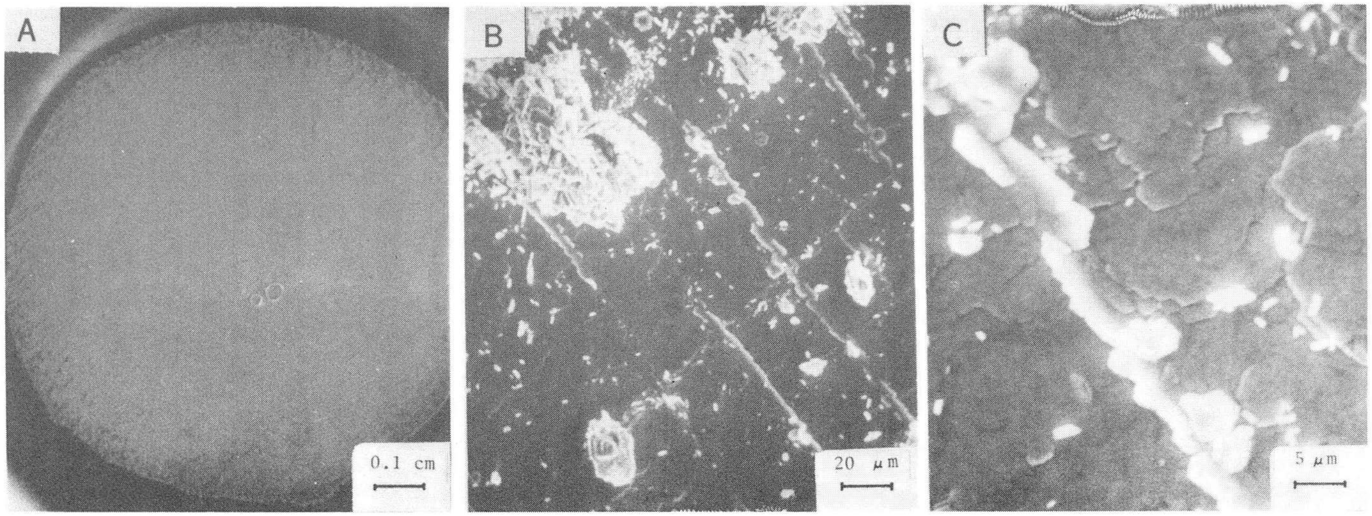

XBB 823-1929

Fig. 11

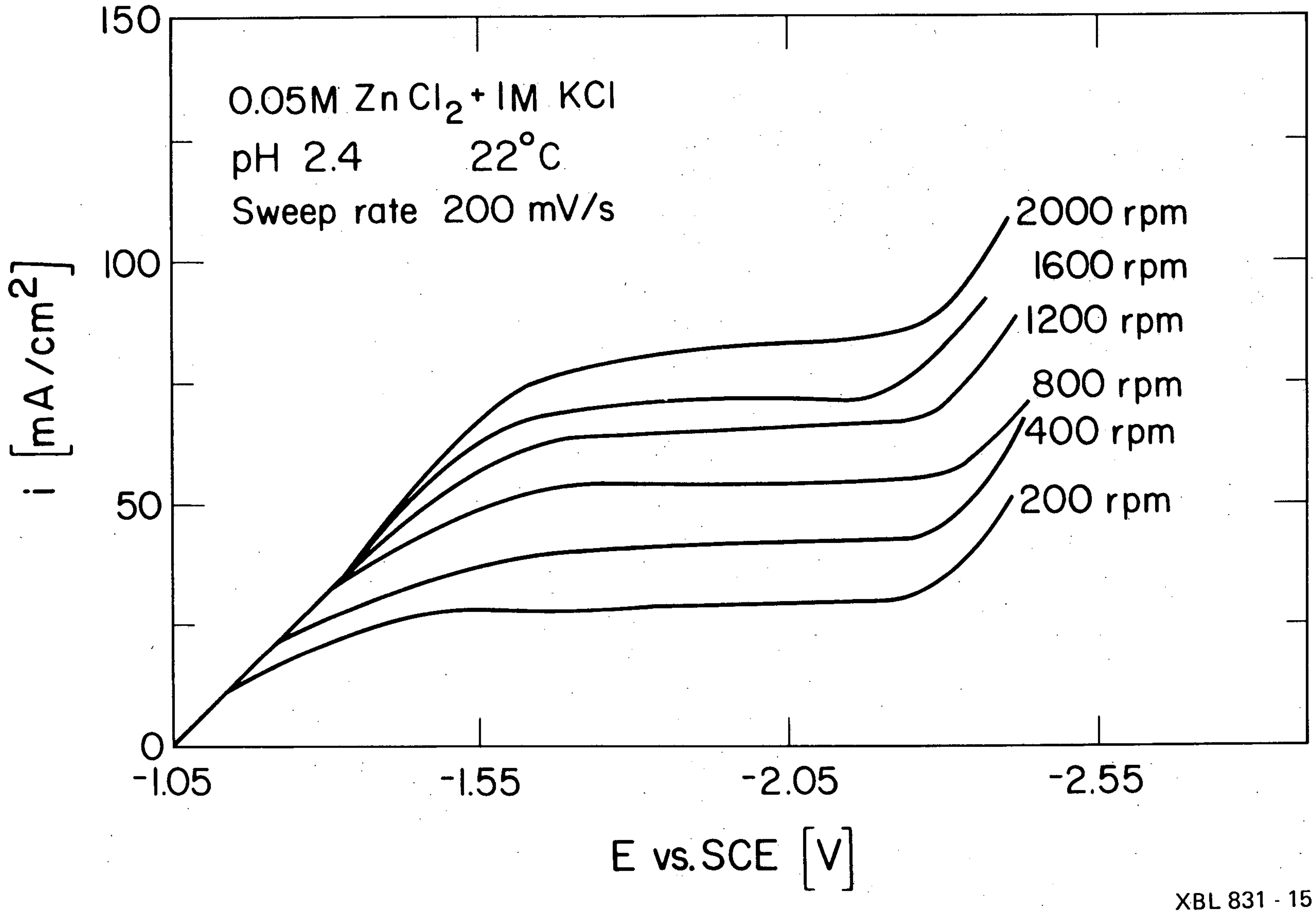
0.05M ZnCl2 + 1M KCl
pH 2.4
22°C
Sweep rate 200 mV/s
2000 rpm
1600 rpm
1200 rpm
800 rpm
400 rpm
200 rpm
150
100
50
0
-1.05
-1.55
-2.05
-2.55
i [mA/cm2]
E vs. SCE [V]
XBL 831 - 15

Fig. 12

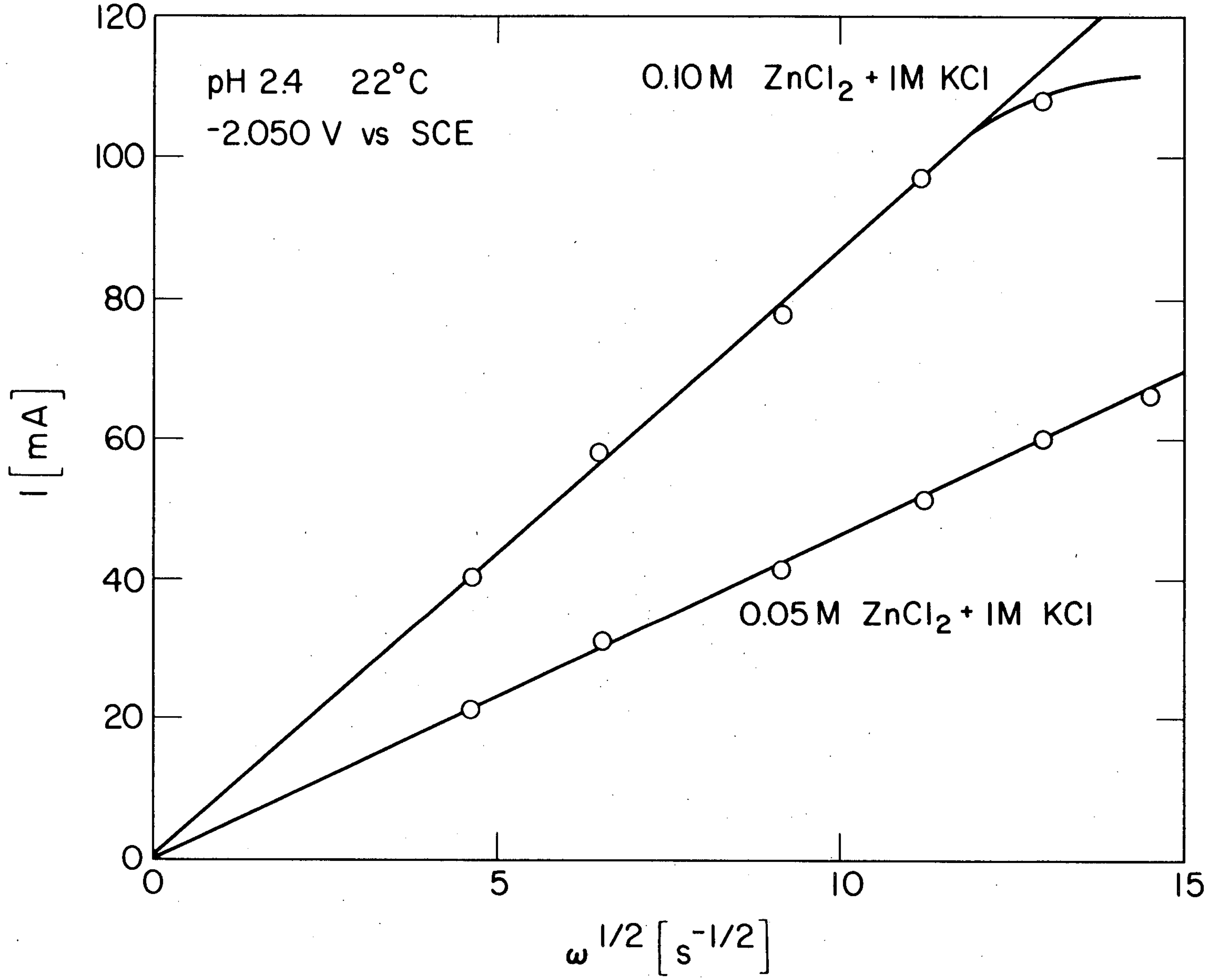

Fig. 13

XBL 831-1050

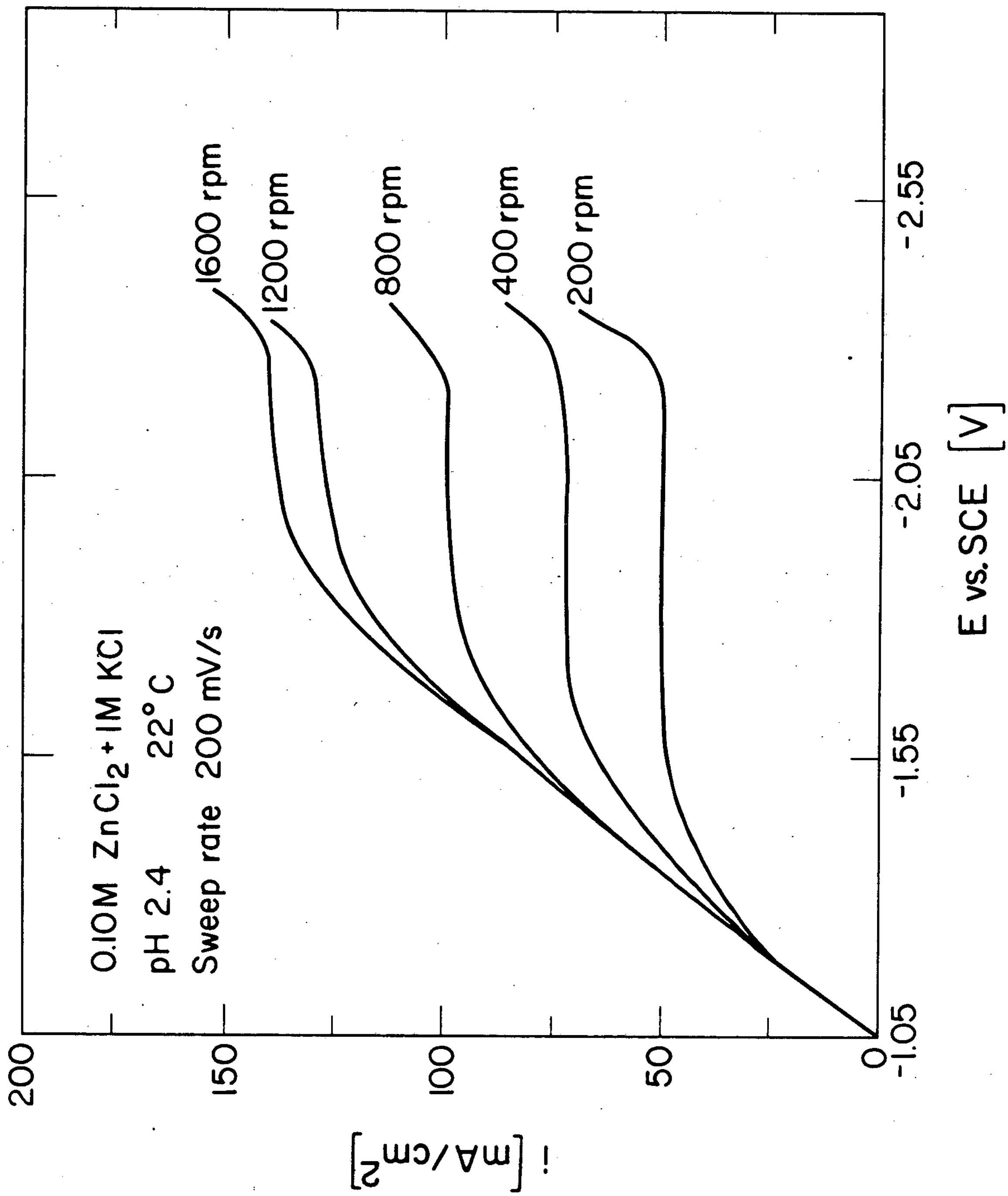

XBL 831-16

Fig. 14

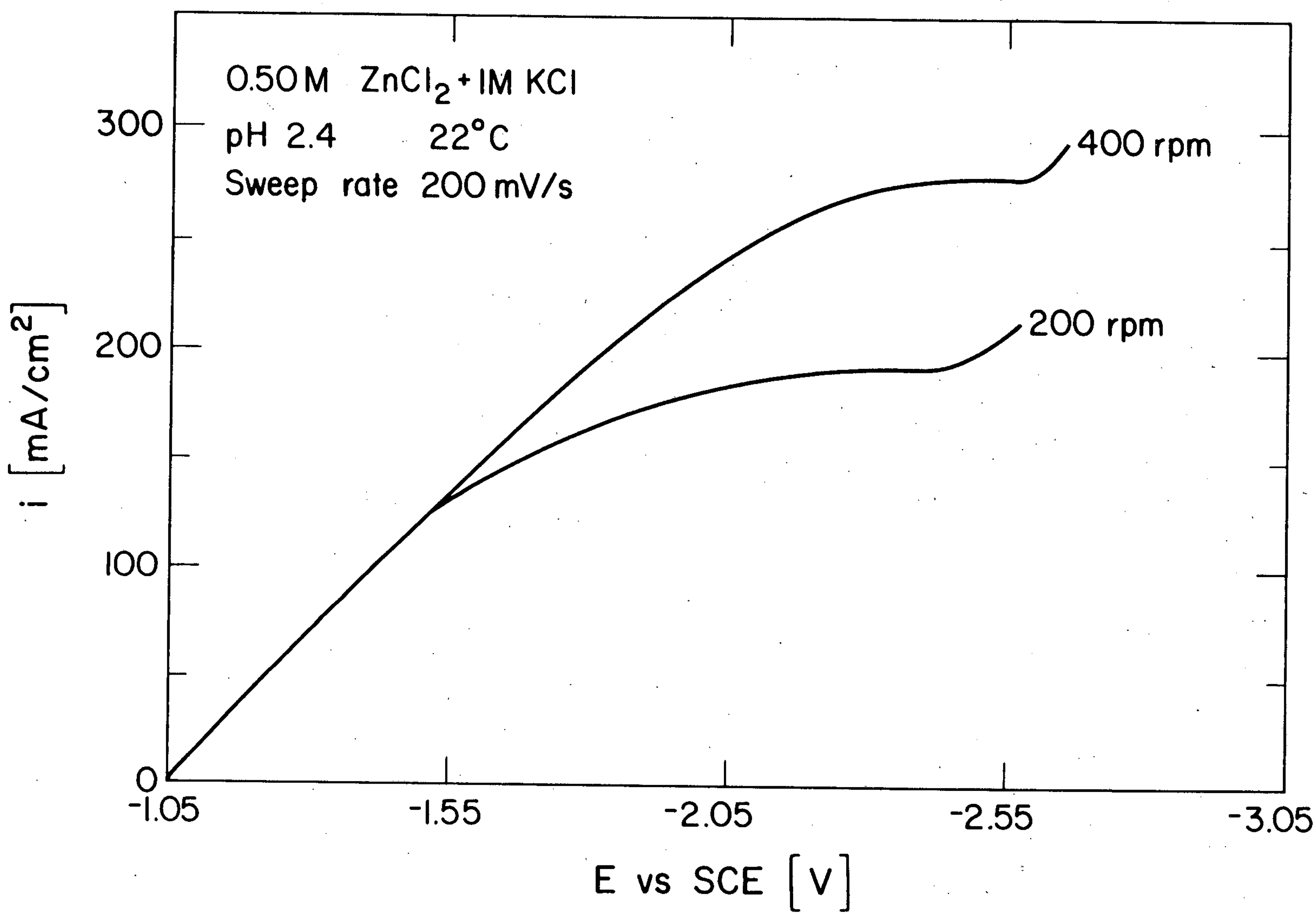

Fig. 15

XBL 831-1051

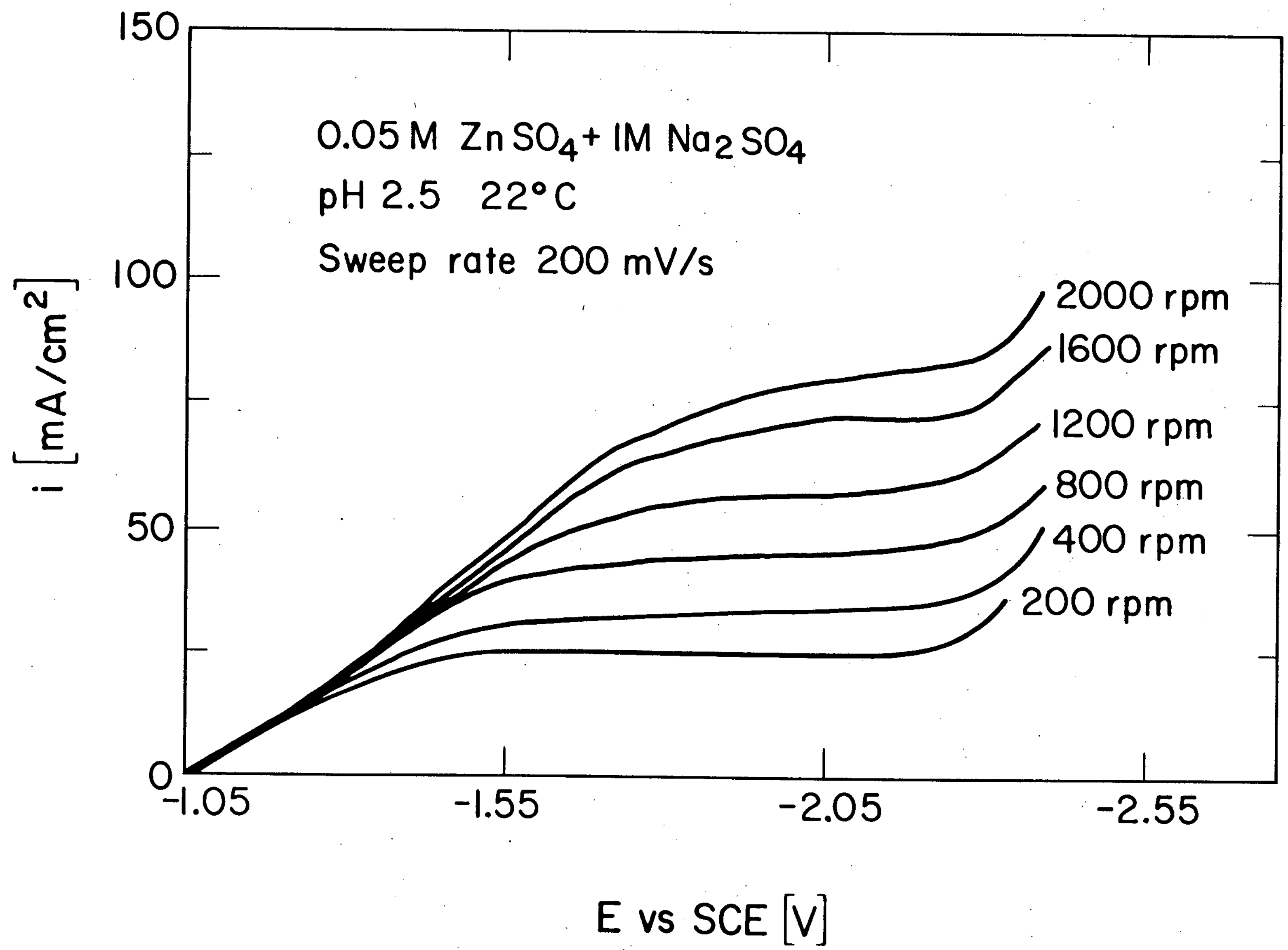

Fig. 16

XBL 831-1041

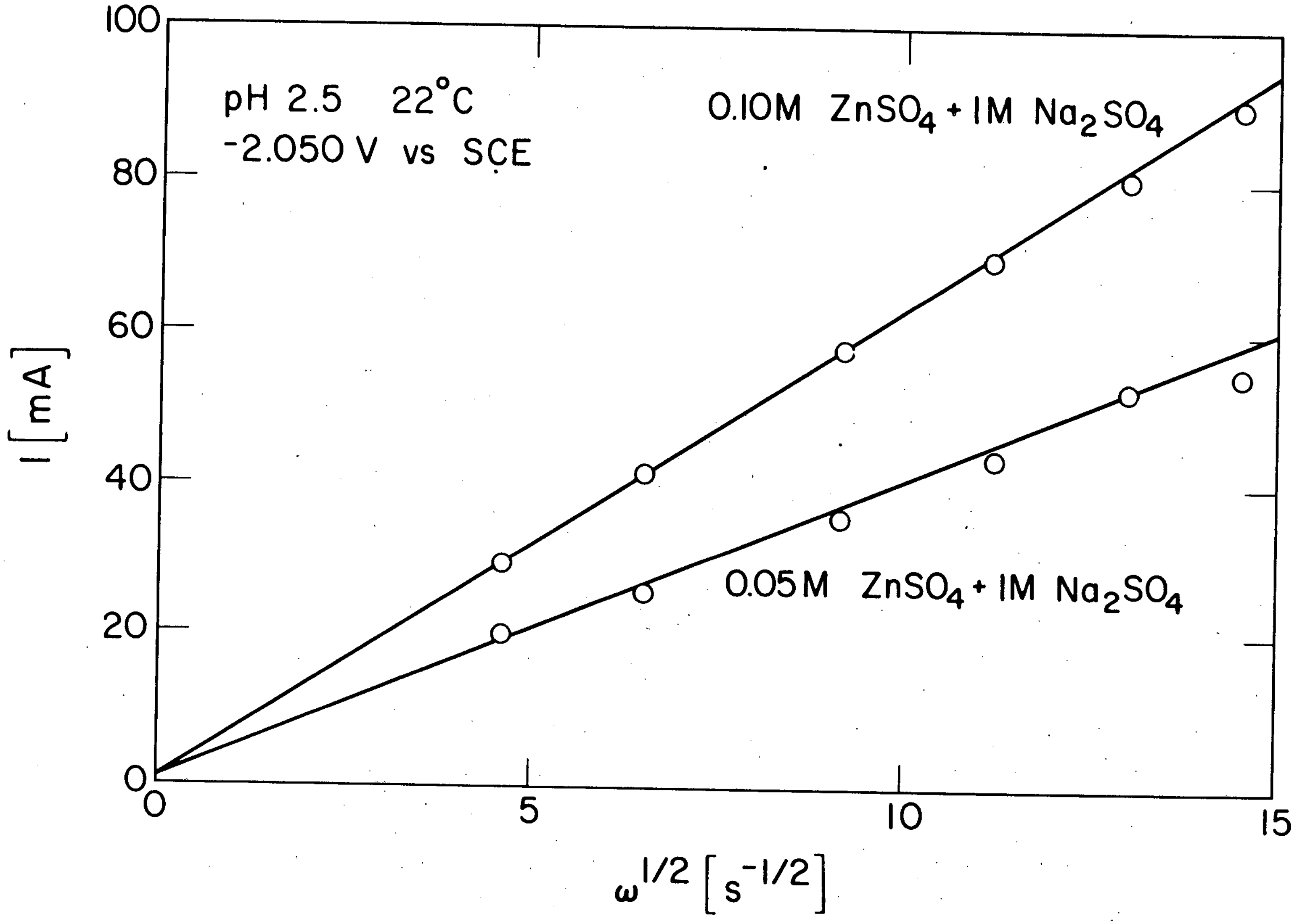

Fig. 17

XBL 831-1047

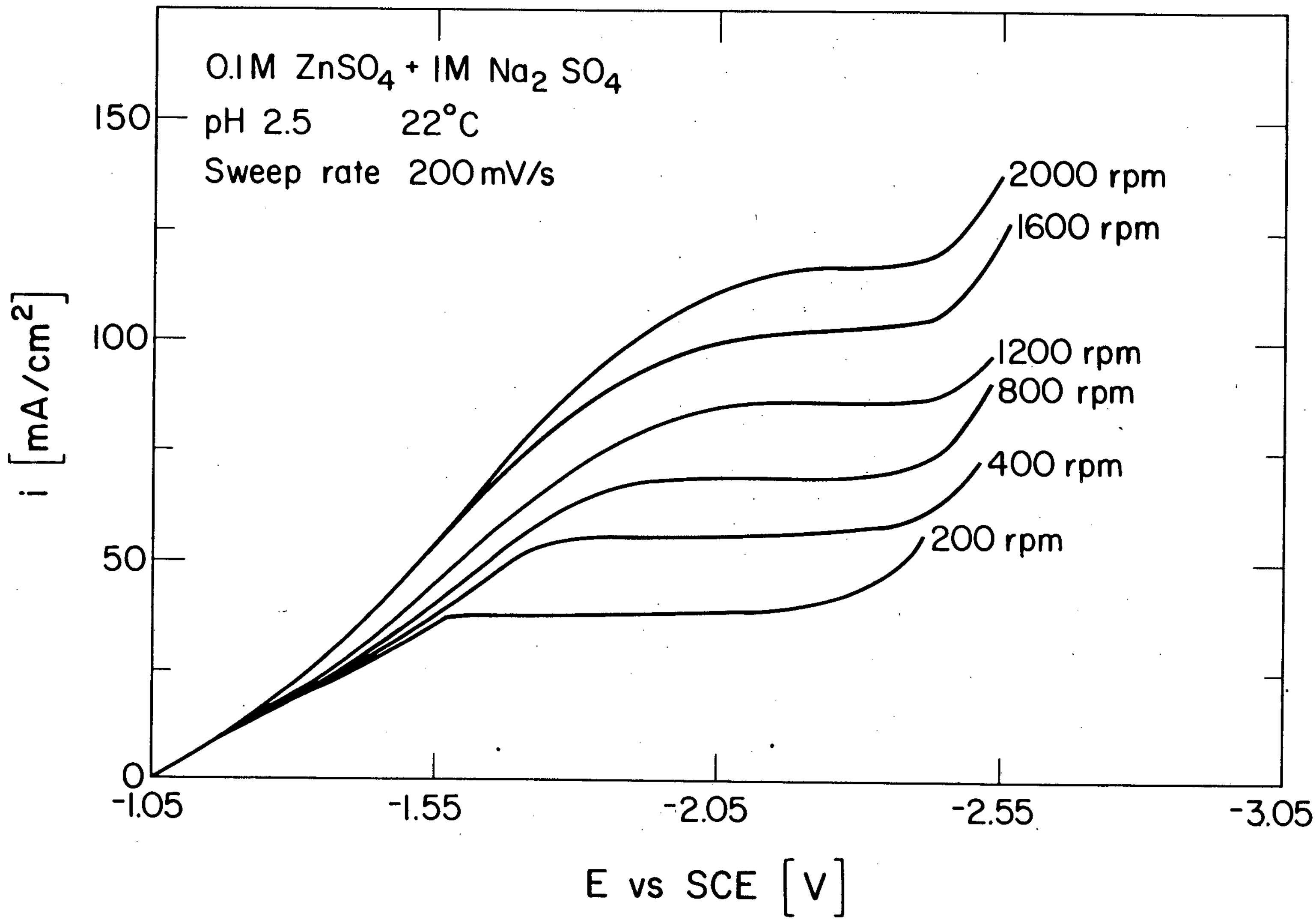

Fig. 18

XBL 831-1039

Table 1. Experimental Data and Results for Deposition of Zinc from $ZnCl_2$ + 1 M KCl Solution

Expt.	$ZnCl_2$ Conc. M	i_L mA/cm^2	k x10^{-3} cm/sec	D x10^{-5} cm^2/sec	Ω rpm	Sweep Rate mV/sec	ν x10^{-2} cm^2/sec	Sc	Re
1	0.05	15.3	1.6	0.419	200	10	0.9969	2380	525
2	0.05	12.9	1.3	0.324	200	10	0.9969	3080	525
3	0.05	20.2	2.1	0.376	400	10	0.9969	2650	1050
4	0.05	20.9	2.2	0.399	400	10	0.9969	2500	1050
5	0.05	28.2	2.9	0.371	800	10	0.9969	2690	2100
6	0.05	26.6	2.8	0.339	800	10	0.9969	2940	2100
7	0.05	34.6	3.6	0.372	1200	10	0.9969	2680	3150
8	0.05	33.0	3.4	0.347	1200	10	0.9969	2870	3150
9	0.05	41.3	4.3	0.388	1600	10	0.9969	2570	4200
10	0.05	37.9	3.9	0.343	1600	10	0.9969	2910	4200
11	0.05	44.3	4.6	0.367	2000	10	0.9969	2720	5250
12	0.05	41.9	4.3	0.337	2000	10	0.9969	2960	5250
13	0.05	25.8	2.7	0.916	200	100	0.9969	1090	525
14	0.05	22.5	2.3	0.746	200	100	0.9969	1340	525
15	0.05	24.2	2.5	0.832	200	100	0.9969	1220	525
16	0.05	26.8	2.8	0.966	200	200	0.9969	1030	525
17	0.05	28.0	2.9	1.032	200	200	0.9969	970	525
18	0.05	38.2	4.0	0.980	400	200	0.9969	1020	1050
19	0.05	40.8	4.3	1.081	400	200	0.9969	920	1050
20	0.05	53.5	5.5	0.965	800	200	0.9969	1030	2100
21	0.05	53.5	5.5	0.965	800	200	0.9969	1030	2100
22	0.05	65.0	6.7	0.953	1200	200	0.9969	1050	3150
23	0.05	63.7	6.6	0.925	1200	200	0.9969	1080	3150
24	0.05	80.3	8.3	1.055	1600	200	0.9969	940	4200
25	0.05	73.9	7.7	0.932	1600	200	0.9969	1070	4200
26	0.05	85.4	8.8	0.979	2000	200	0.9969	1020	5250
27	0.05	82.8	8.6	0.935	2000	200	0.9969	1070	5250
28	0.10	48.4	2.5	0.846	200	200	1.011	1200	518
29	0.10	53.5	2.8	0.983	200	200	1.011	1030	518
30	0.10	79.0	4.1	1.033	400	200	1.011	980	1036
31	0.10	70.1	3.6	0.878	400	200	1.011	1150	1036
32	0.10	98.1	5.1	0.850	800	200	1.011	1190	2072
33	0.10	98.1	5.1	0.850	800	200	1.011	1190	2072
34	0.10	118.5	6.1	0.832	1200	200	1.011	1220	3108
36	0.10	124.8	6.5	0.914	1200	200	1.011	1110	3108
37	0.10	137.6	7.1	0.854	1600	200	1.011	1180	4144
38	0.10	99.1	5.1	0.877	800	100	1.011	1150	2072
39	0.50	191.0	2.0	0.593	200	200	1.080	1820	485
40	0.50	188.0	1.9	0.580	200	200	1.080	1860	485
41	0.50	188.0	1.9	0.580	200	200	1.080	1860	485
42	0.50	265.0	2.7	0.577	400	200	1.080	1870	970
43	0.50	268.0	2.8	0.584	400	200	1.080	1850	970

Table 2. Experimental Data and Results for Deposition of Zinc from $ZnSO_4$ + 1 M Na_2SO_4 Solution

Expt.	$ZnSO_4$ Conc. M	i_L mA/cm^2	k $\times 10^{-3}$ cm/sec	D $\times 10^{-5}$ cm^2/sec	Ω rpm	Sweep Rate mV/sec	ν $\times 10^{-2}$ cm^2/sec	Sc	Re
1	0.05	24.2	2.5	0.852	200	100	1.112	1310	471
2	0.05	22.9	2.4	0.785	200	200	1.112	1420	471
3	0.05	34.4	3.6	0.860	400	100	1.112	1290	942
4	0.05	31.8	3.3	0.765	400	100	1.112	1450	942
5	0.05	31.8	3.3	0.765	400	200	1.112	1450	942
6	0.05	45.9	4.8	0.788	800	100	1.112	1410	1884
7	0.05	45.9	4.8	0.788	800	100	1.112	1410	1884
8	0.05	44.6	4.6	0.755	800	200	1.112	1470	1884
9	0.05	54.8	5.7	0.758	1200	100	1.112	1470	2826
10	0.05	54.8	5.7	0.758	1200	200	1.112	1470	2826
11	0.05	67.5	7.0	0.836	1600	100	1.112	1330	3768
12	0.05	66.2	6.9	0.812	1600	100	1.112	1370	3768
13	0.05	63.7	6.6	0.766	1600	200	1.112	1450	3768
14	0.05	71.3	7.4	0.768	2000	100	1.112	1450	4710
15	0.05	68.8	7.1	0.728	2000	100	1.112	1530	4710
16	0.10	36.9	1.9	0.569	200	200	1.118	1960	468
17	0.10	36.9	1.9	0.569	200	200	1.118	1960	468
18	0.10	34.4	1.8	0.512	200	100	1.118	2180	468
19	0.10	53.5	2.8	0.590	400	200	1.118	1890	936
20	0.10	53.5	2.8	0.590	400	200	1.118	1890	936
21	0.10	53.5	2.8	0.590	400	200	1.118	1890	936
22	0.10	73.9	3.8	0.570	800	200	1.118	1960	1872
23	0.10	75.2	3.9	0.585	800	200	1.118	1910	1872
24	0.10	71.3	3.7	0.540	800	200	1.118	2070	1872
25	0.10	89.2	4.6	0.558	1200	200	1.118	2000	2808
26	0.10	89.2	4.6	0.558	1200	200	1.118	2000	2808
27	0.10	89.2	4.6	0.558	1200	200	1.118	2000	2808
28	0.10	101.9	5.3	0.548	1600	200	1.118	2040	3744
29	0.10	103.2	5.3	0.599	1600	200	1.118	1870	3744
30	0.10	114.6	5.9	0.554	2000	200	1.118	2020	4680
31	0.10	114.6	5.9	0.554	2000	200	1.118	2020	4680

Table 3. Comparison of Diffusion Coefficients of Zinc with Literature Data

(D in 10^{-5} cm^2/sec)

Reference	Solution	Method	Temp. (^oC)	pH	Concentrations (M)						
					0.05	0.1	0.2	0.4	0.5	1.0	1.6
Present Study	$ZnCl_2$ + 1 M KCl	RDE	22	2.4	0.98	0.89			0.58		
5	$ZnCl_2$ + 1 M KCl	RDE	25		0.89						
7	$ZnCl_2$ + 3.5 M KCl	Capillary	26.5					0.82			0.88
8	$ZnCl_2$ + 3 M KCl	Polarography	25	3.5		0.52			0.45	0.41	
10	$ZnCl_2$	Interferometry	25				1.027	1.007			
12	$ZnCl_2$	Interferometry	25		1.048						
15	$ZnCl_2$	Interferometry	25					1.003	0.991		
Present Study	$ZnSO_4$ + 1 M Na_2SO_4	RDE	22	2.5	0.78	0.57					
11	$ZnSO_4$	Interferometry	25		0.60	0.56	0.51		0.43	0.37	

TECHNICAL INFORMATION DEPARTMENT
LAWRENCE BERKELEY LABORATORY
UNIVERSITY OF CALIFORNIA
BERKELEY, CALIFORNIA 94720